

DOE/JPL 954334-78/8
Distribution Category UC-63



QUARTERLY PROGRESS REPORT

July-September 1978

Low cost silicon solar array project

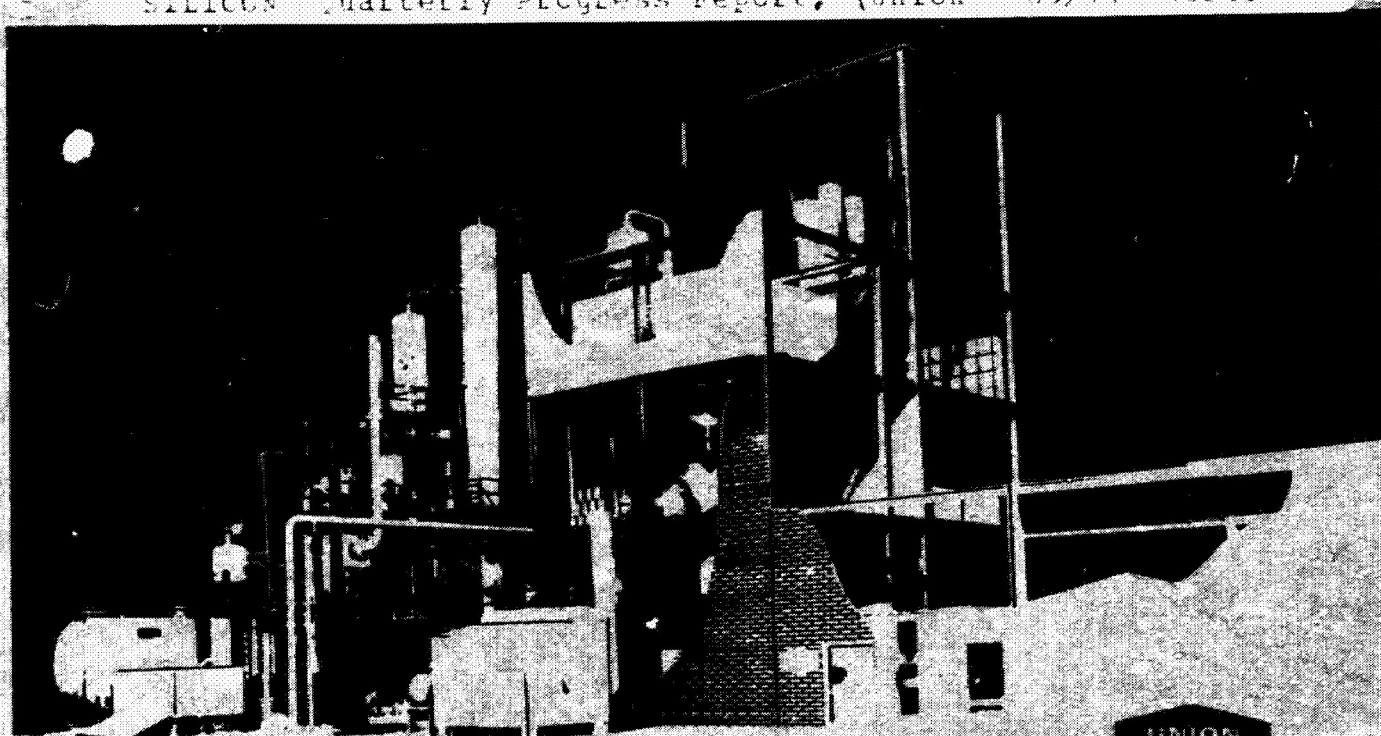
FEASIBILITY OF LOW-COST, HIGH-VOLUME PRODUCTION OF SILANE
AND PYROLYSIS OF SILANE TO SEMICONDUCTOR-GRADE SILICON

(NASA-CF-158097) LOW COST SILICON SOLAR
ARRAY PROJECT: FEASIBILITY OF LOW-COST,
HIGH-VOLUME PRODUCTION OF SILANE AND
PYROLYSIS OF SILANE TO SEMICONDUCTOR-GRADE
SILICON Quarterly Progress Report, (Union

N79-16376

Inclas

63/44 43638



UNION CARBIDE
CORPORATION

THE JPL LOW-COST SILICON SOLAR ARRAY PROJECT IS SPONSORED BY THE U.S. DEPARTMENT OF ENERGY AND FORMS PART OF THE SOLAR PHOTOVOLTAIC CONVERSION PROGRAM TO INITIATE A MAJOR EFFORT TOWARD THE DEVELOPMENT OF LOW-COST SOLAR ARRAYS. THIS WORK WAS PERFORMED FOR THE JET PROPULSION LABORATORY, CALIFORNIA INSTITUTE OF TECHNOLOGY BY AGREEMENT BETWEEN NASA AND DOE.

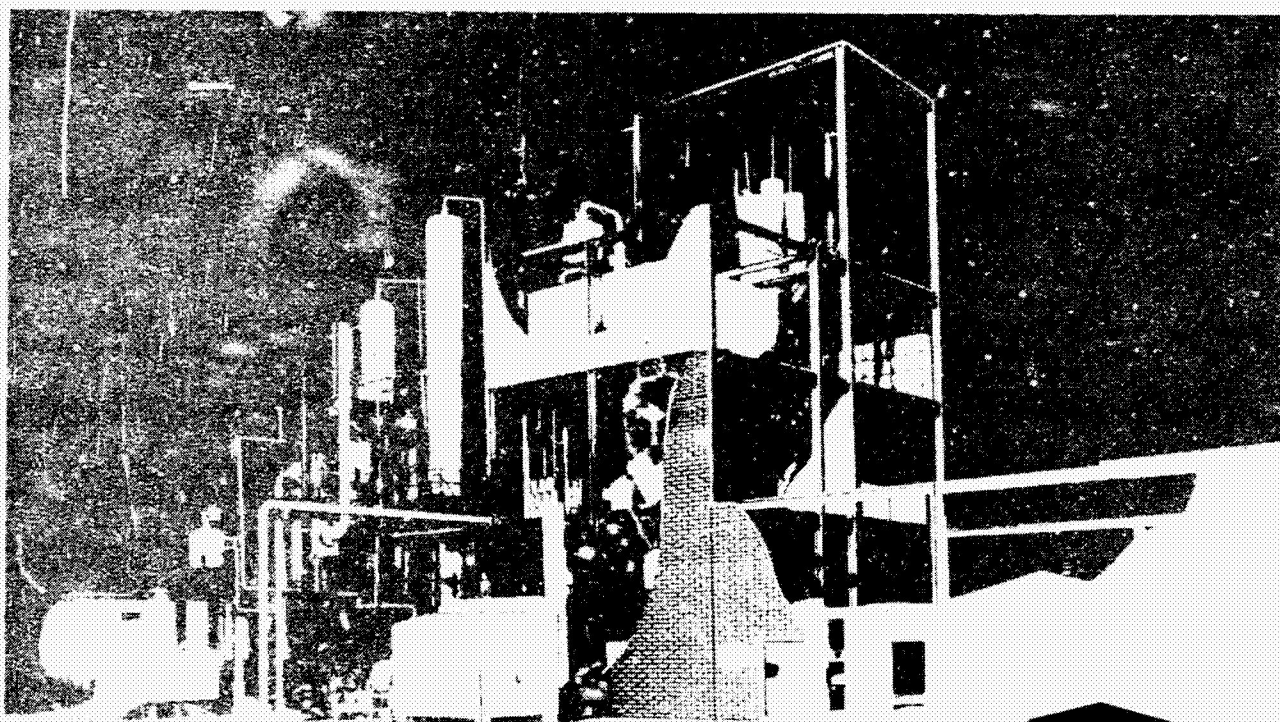
DOE/JPL 954334-78/8
Distribution Category UC-63

QUARTERLY PROGRESS REPORT

July-September 1978

low cost silicon solar array project

FEASIBILITY OF LOW-COST, HIGH-VOLUME PRODUCTION OF SILANE
AND PYROLYSIS OF SILANE TO SEMICONDUCTOR-GRADE SILICON



W.C. Breneman E.G. Farrier H. Morihara

UNION CARBIDE
CORPORATION

TABLE OF CONTENTS

	PAGE NO.
ABSTRACT	1
1.0 SILANE PRODUCTION	2
1.1 INTRODUCTION	2
1.2 DISCUSSION	4
1.2.1 PROCESS DEVELOPMENT	4
1.2.1.1 SILANE PRODUCT QUALITY	4
1.2.1.2 CATALYST LONGEVITY	6
1.2.2 H_2SiCl_2 DISPROPORTIONATION	7
1.2.3 HYDROGENATION KINETICS	14
1.2.4 SILANE, PHOSPHINE, DIBORANE EQUILIBRIA	16
1.2.5 MATERIALS of CONSTRUCTION	18
1.3 CONCLUSIONS	19
1.4 PROJECTED QUARTERLY ACTIVITIES	20
1.5 REFERENCES	20
 2.0 SILICON PRODUCTION	 21
2.1 INTRODUCTION	21
2.2 DISCUSSION	22
2.2.1a FLUID BED REACTOR	22
2.2.1b FREE SPACE REACTOR	25
2.2.1c SILICON POWDER TRANSFER	27
2.2.1d SILICON CONSOLIDATION	27
2.2.1e SUPPORTING ACTIVITIES	29
2.3 CONCLUSIONS	30
2.4 PROJECTED FOURTH QUARTER 1978 ACTIVITIES	32
2.4.1 FLUID BED REACTOR	32
2.4.2 FREE SPACE REACTOR	32
2.4.3 SILICON POWDER CONSOLIDATION	32
 3.0 PROCESS DESIGN	 34
3.1 INTRODUCTION	34
3.2 DISCUSSION	36
3.2.1 SGS PROCESS DESIGN for the 100 MT/Yr EPSDU	36
3.2.1a HEAT and MASS BALANCE	36

TABLE OF CONTENTS (Cont'd)

	PAGE NO.
3.2.1b PYROLYSIS SYSTEM DESIGN	39
3.2.1c PIPING and INSTRUMENTATION WORKSHEETS	41
3.2.1d WASTE DISPOSAL TESTING	41
3.2.1e ADSORPTION SYSTEM DESIGN	42
3.2.2 PROCESS DESIGN DATA and MODELING	45
3.2.2a DATA ACQUISITION	45
3.2.2b CHEMICAL EQUILIBRIUM and HEATS of FORMATION	47
3.2.2c REDISTRIBUTION RATE CONSTANTS	52
3.2.3 OTHER ACTIVITIES	52
3.2.3a ENGINEERING PRACTICES PACKAGE	52
3.2.3b PRODUCT SAMPLE ANALYSIS	52
3.2.3c EQUIPMENT VENDOR IDENTIFICATION	52
3.2.3d PROCESS SYSTEM VALVING and PIPING	52
3.3 CONCLUSIONS	54
3.4 PROJECTED QUARTERLY ACTIVITIES	55
3.4.1 HEAT and MASS BALANCE	55
3.4.2 PFD and STREAM CATALOG	55
3.4.3 FUNCTIONAL EQUIPMENT SPECIFICATIONS	55
3.4.4 KEY EQUIPMENT DESIGN	55
3.4.5 WASTE DISPOSAL TESTING	55
3.4.6 P&I DIAGRAM	56
3.4.7 MAJOR EQUIPMENT COSTING	56
3.4.8 PYROLYSIS SYSTEM DESIGN	56
3.5 REFERENCES	57
 4.0 FLUID-BED PYROLYSIS R&D	 58
4.1 INTRODUCTION	58
4.2 DISCUSSION	59
4.2.1 THEORETICAL INVESTIGATIONS	59
4.2.1a FLUID-BED SCALING LAWS	59
4.2.1b FIXED-BED PYROLYSIS MODELING	61
4.2.2 EXPERIMENTAL WORK	65
4.2.2a HIGH-TEMPERATURE FLUID-BED	65
4.2.2b COLD MODELING EXPERIMENTS	65

TABLE OF CONTENTS (Cont'd)

	PAGE NO.
4.2.2c PARTICLE ATTRITION TEST	68
4.2.3 INTERIM TECHNICAL SUMMARY	71
4.3 CONCLUSIONS	75
4.4 PROJECTED QUARTERLY ACTIVITIES	76
4.4.1 THEORETICAL INVESTIGATIONS	76
4.4.1a FLUID-BED PYROLYSIS MODEL UPDATE	76
4.4.1b FIXED-BED PYROLYSIS MODELING	76
4.4.2 EXPERIMENTAL WORK	77
4.4.2a HIGH-TEMPERATURE FLUID-BED	77
4.4.2b COLD MODELING EXPERIMENTS	77
4.4.2c GAS DISTRIBUTOR TEST	77
4.4.2d PARTICLE ATTRITION TEST	77
4.5 REFERENCES	78

LIST OF ILLUSTRATIONS

TABLES

TABLE NO.		PAGE NO.
1.1	ANALYSIS of SILANE	5
1.2	NITROGEN CONTENT of AMBERLYST A-21 RESIN in CHLOROSILANE REDISTRIBUTION	7
1.3	DICHLOROSILANE EQUILIBRIUM LIQUID vs. VAPOR PHASE DISPROPORTIONATION at 50–60°C	8
1.4	HYDROGENATION in 3" FLUID BED REACTOR	15
3.1	PURE COMPONENT VAPOR PRESSURE	46
3.2	DEFINITION of TERMS in EXPERIMENTAL RAW DATA TABLES	48
3.3	EXPERIMENTAL DATA N_2 , CH_4 , CO_2 , and HCl in DICHLOROSILANE	49
3.4	EXPERIMENTAL DATA N_2 , CH_4 , CO_2 , and HCl in TRICHLOROSILANE	50
3.5	EXPERIMENTAL DATA N_2 , CH_4 , CO_2 , and HCl in TETRACHLOROSILANE	51

FIGURE NO.

FIGURES

1.1	CONCENTRATION of SILANE vs. RESIDENCE TIME, DICHLOROSILANE REDISTRIBUTION	10
1.2	CONCENTRATION of MONOCHLOROSILANE vs. RESIDENCE TIME, DICHLOROSILANE REDISTRIBUTION	11
1.3	CONCENTRATION vs. RESIDENCE TIME, DICHLOROSILANE REDISTRIBUTION	12
1.4	CONCENTRATION of TRICHLOROSILANE vs. RESIDENCE TIME, DICHLOROSILANE REDISTRIBUTION	13
1.5	SILANE VAPOR/LIQUID EQUILIBRIUM CELL	17
2.1	CROSS-SECTION of COATED SEED PARTICLES (500X)	24
2.2	COATING on SILICON SEED PARTICLES in the AGGLOMERATED PLUG (100X)	24
2.3	SCANNING ELECTRON MICROGRAPH of FREE SPACE REACTOR SILICON POWDER (5000X)	28
2.4	SCANNING ELECTRON MICROGRAPH of LOOSE SILICON POWDER SINTERED UNDER VACUUM for ONE HOUR at 1300°C (5000X)	28
2.5	SCANNING ELECTRON MICROGRAPH of SILICON FLAKE SINTERED UNDER VACUUM for ONE HOUR at 1350°C (50X)	31
3.1	FLOWSHEET of APPARATUS for HYDROLYSIS and LIME NEUTRALIZATION of SILICON TETRACHLORIDE	43
3.2	ADSORPTION SYSTEM FLOWSHEET	44
4.1	PRESSURE DROP vs. FLOWRATE for –35/+60 MESH LEAD PARTICLES FLUIDIZED by HELIUM in a 2" DIAMETER COLUMN	66
4.2	PRESSURE DROP vs. FLOWRATE for +35 MESH LEAD PARTICLES FLUIDIZED by HELIUM in a 2" DIAMETER COLUMN	67
4.3	PRESSURE DROP vs. FLOWRATE for –120/+200 MESH LEAD PARTICLES FLUIDIZED by HELIUM in a 6" DIAMETER COLUMN by 1' COLUMN	69
4.4	PRESSURE DROP vs. VELOCITY for –60/+120 MESH SILICON FLUIDIZED by HELIUM in a 6" DIAMETER by 1' COLUMN	70
4.5	RATE of FINES GENERATED for –35/+60 METALLURGICAL SILICON PARTICLES vs. TIME, at $U/U_{mf} = 10$, MASS of SILICON in BED = 35 GRAMS	72
4.6	RATE of FINES GENERATION for –35/+60 SEMICONDUCTORS GRADE SILICON PARTICLES at $U/U_{mf} = 5$, MASS of SILICON in BED = 35 GRAMS	73

ABSTRACT

SILANE PRODUCTION

Silicon epitaxy analysis of silane produced in the Process Development Unit operating in a completely integrated mode consuming only hydrogen and metallurgical silicon resulted in film resistivities of up to 120 ohms cm N type. Preliminary kinetic studies of dichlorosilane disproportionation in the liquid phase have shown that 11.59% SiH_4 is formed at equilibrium after 12 minutes contact time at 56°C. Hydrogenation of silicon tetrachloride at 500°C in a 3 inch fluid-bed reactor at 100 psi produced trichlorosilane in yields predicted from laboratory data. Corrosion tests indicate Incoloy 800 is preferred over stainless steel for construction of the hydrogenation reactor.

SILICON PRODUCTION

The fluid-bed reactor was operated continuously for 48 hours with a mixture of one percent silane in helium as the fluidizing gas. A high silane pyrolysis efficiency was obtained without the generation of excessive fines. Gas flow conditions near the base of the reactor were unfavorable for maintaining a bubbling bed with good heat transfer characteristics. Consequently, a porous agglomerate formed in the lower portion of the reactor. Dense coherent plating was obtained on the silicon seed particles which had remained fluidized throughout the experiment.

The free-space reactor was operated for eight (8) consecutive silane pyrolysis experiments, at a silicon production rate of 0.45 kg/hr, without dismantling or servicing the reactor. The silicon powder was pneumatically transferred from the settling chamber, located beneath the reactor, to a larger capacity storage hopper. The reactor will be operated for additional consecutive runs before the system is dismantled for inspection.

Several methods were investigated for converting the free-space reactor powder into a more suitable feedstock for silicon melters. Loose powder sintering did not densify the powder sufficiently. Powder compacts formed by conventional dry pressing and sintering had sufficient density and strength; and, although some delaminations occurred, this product should be acceptable. Direct rolled flakes of the free-space reactor powder densified more than anticipated during sintering. The higher density may have been promoted by the introduction of transition metals during the rolling operation. Additional work will be necessary to minimize contamination.

An analytical model for the fixed-bed pyrolysis was generated in a form of partial differential equations. They will be solved by a finite difference method. The model should predict behavior of fixed-bed pyrolysis.

Basic fluid bed behavior study is in progress using 2- and 6-inch diameter cold beds. Lead and silicon particles are fluidized by air, helium or hydrogen. According to Dr. T. Fitzgerald, lead particles fluidized by helium at room temperature can model silicone particles at 900°C fluidized by a mixture of hydrogen and silane. This will be verified in the next quarter.

Attrition tests are conducted to determine if fluid bed seed particles can be produced by fluidizing silicon particles at a high U/U_{mf} and generating fines. It appears that high purity silicon will produce more fines than metallurgical-grade silicon.

PROCESS DESIGN

Process Design work in progress for the Experimental Process System Development Unit (EPSDU) sized for 100 MT/Yr includes free-space pyrolysis reactor and melter design, and a heat and mass balance, where recently acquired experimental vapor-liquid equilibrium data and available open literature data for chlorosilanes and its impurities have been successfully modeled.

A preliminary piping and instrumentation diagram for the EPSDU was prepared for all sections except the waste treatment and the pyrolysis process. It is suitable to generate P&I diagrams. Most of the necessary process design data were obtained during this reporting period. The VLE data of B_2H_6 , PH_3 , and AsH_3 in silane is yet to be measured. This work will be completed in October.

A computer program has been written that determines rate constants for the three simultaneous redistribution reactions. A small bench-scale waste disposal testing apparatus has been designed for testing the feasibility of sludge treatment by acid hydrolysis and lime neutralization. The apparatus is under construction.

1.0 SILANE PRODUCTION

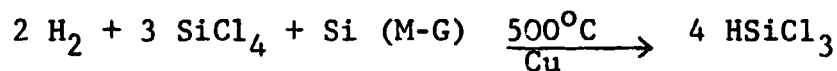
1.1 Introduction

The purpose of this program is to determine the feasibility and practicality of high-volume, low-cost production of silane (SiH_4) as an intermediate for obtaining solar-grade silicon metal. The process is based on the synthesis of SiH_4 by the catalytic disproportionation of chlorosilanes resulting from the reaction of hydrogen, metallurgical silicon, and silicon tetrachloride. The goal is to demonstrate the feasibility of a silane production cost of under \$4.00/kg at a production rate of 1000 MT/year.

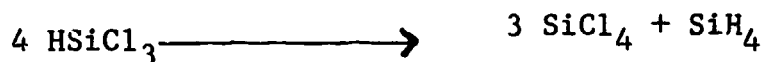
Prior to the inception of this program in October 1975, Union Carbide had shown that pure hydrochlorosilanes could be disproportionated to an equilibrium mixture of other hydrochlorosilanes by contact with a tertiary-amine, ion-exchange resin. In addition, Union Carbide had shown that silicon tetrachloride, a by-product of silane disproportionation, can be converted to trichlorosilane by reaction with metallurgical silicon metal and hydrogen.

Thus, a closed-cycle purification scheme was proposed to convert metallurgical-grade silicon into high-purity, solar-grade silicon using hydrochlorosilanes as intermediates. This process appears as:

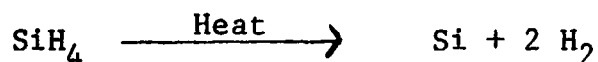
1. Hydrogenation of metallurgical silicon metal and of by-product silicon tetrachloride to form trichlorosilane.



2. Disproportionation of trichlorosilane to silane and silicon tetrachloride.



3. Pyrolysis of silane to high-purity silicon.



Until now, laboratory investigations have defined the rate, equilibrium conversion, and certain mechanistic aspects of the disproportionation and hydrogenation reactions at atmospheric pressure. A small process development unit (PDU), capable of operating under pressure, was constructed and operated to demonstrate the conversion of dichlorosilane to silane. A high-pressure hydrogenation unit was constructed and the kinetics of the hydrogenation reaction were studied at elevated pressures. An integrated process development unit to demonstrate the closed cycle production of silane from metallurgical Si and H₂ was designed and constructed incorporating both the high pressure hydrogenation and redistribution reactor systems. The integrated production of silane was achieved in the process development unit, and 3.2 kg of high purity silane were made. Experiments were started to obtain SiCl₄ hydrogenation and H₂SiCl₂ disproportionation kinetic data at the latest design conditions of Union Carbide's Experimental Process System Development Unit sized for 100 MT/year of Silicon.

1.2 Discussion

1.2.1 Process Development

1.2.1.1 Silane Product Quality

Analysis of the 3.2 kg of silane produced last period⁽²⁾ in the integrated Process Development Unit, PDU, showed it to be substantially free of electronically active materials, to contain small quantities of other silicon compounds, and modest amounts of inert gas and hydrogen. (Table 1.1).

The electronic quality of the silane was determined by a standard epitaxial deposition of a 10 micron film on 6 μ cm boron doped silicon wafer. Resistivity measured with a four point probe showed 20 and 120 μ cm N type deposits with less than 10% variation across the wafer. Visual examination showed no unusual defects, pits, etc. The wafers appeared equivalent to those prepared from commercial quality silane.

The level of helium and hydrogen in the silane is somewhat uncertain as they could not be independently resolved on existing analytical equipment. The presence of helium is not unexpected since it is used as the inerting gas in the PDU and steps are not taken to assure its complete removal.

Table 1.1

ANALYSIS OF SILANE

Cylinder Number	LK 290145	LK 290044
Cylinder Pressure, psig	275	325
Hydrogen*	14.37	15.05
Helium*	35.9	36.6
Nitrogen %	2.03	2.56
DiSilane, ppm	66	53
TriSilane	83	75
TetraSilane	71	144
Siloxane	35	53
Monochlorosilane	51	31
Dichlorosilane	< 8	< 8
Trichlorosilane	217	81
Silicon Tetrachloride	70	60
Methyl Silane	99	91
Methane	< 50	< 50
Epitaxy		
Resistivity, Ω cm	20	120
Type	N	N

* H₂ and He were not able to be independently determined.

Nitrogen is used as the inerting gas in the hydrogenation reactor section of the PDU. Carry forward into the silane reactor section of a small amount, soluble in the $\text{SiCl}_4/\text{HSiCl}_3$ feed, was expected. The EPSDU design provides for degassing of the hydrogenation reactor product which would eliminate these and other permanent gas impurities.

The presence of polysilanes is noted - is not expected but does not appear to be a problem. The level of chlorosilanes is unexpectedly high. On-line analysis of the purified silane showed less than 10 ppm of trichlorosilane. However, since the carbon adsorption traps were regenerated several times during the run, it is possible that a break through or desorption cycle misvalving could have forced chlorosilanes into the product cylinders.

Recognizing these potential problems, the EPSDU is designed to remove chlorosilanes by distillation instead of by adsorption.

1.2.1.2 Catalyst Longevity

The AMBERLYST A-21 ion exchange resin catalyst used in the disproportionation reactors has been shown to have a long activity. Laboratory tests earlier⁽¹⁾ have indicated stable catalyst reactivity was achieved after an initial 25% decline which was also accompanied by proportional loss of amine functionality. Samples of the resin catalyst from the PDU were analyzed for nitrogen content as an expedient check on resin activity. As shown in Table 1.2, the nitrogen content dropped quickly in the

first eight hours of operation to 77% of the initial value and then much more slowly. A linear extrapolation of the declining nitrogen content indicates a life expectancy of about 1500 hours. However, the data does not show whether the decline is linear or is asymptotic. Previous work had shown no substantial decline in activity after 1600 hours of operation and no noticeable decline in activity has been observed in the PDU after 300 hours.

Table 1.2

**NITROGEN CONTENT OF AMBERLYST A-21 RESIN
IN CHLOROSILANE REDISTRIBUTION**

<u>Cummulative Reaction Time, Hour</u>	<u>Wt. % N</u>
0	6.25
8	4.8
70	4.5
300	3.8

1.2.2 H_2SiCl_2 Disproportionation

Preliminary kinetic and equilibrium data on the disproportionation of chlorosilanes at EPSDU design conditions were obtained. Previous data on the chlorosilane system were measured with vapor phase reactants⁽¹⁾. Processing economics have indicated that the temperature and pressure conditions most suitable would result in liquid chlorosilanes passing

through the fixed bed catalytic reactors.

A laboratory scale packed bed catalytic reactor was constructed to obtain integral type kinetic data for dichlorosilane and trichlorosilane disproportionation. An all liquid system was assured by operating at 600 psi, well above the vapor pressure of the equilibrium mixture at the reactor temperature. The reactor effluent was vaporized at atmospheric pressure and analyzed by an on-line gas chromatograph. Residence times as short as 0.13 and as long as 50 minutes were achieved by altering the catalyst bed depth and dichlorosilane flow rate. For temperatures of 32°C, 55.5°C and 81°C, liquid phase composition versus residence time was measured (Figures 1.1 - 1.4), for dichlorosilane feed.

The data indicate that equilibrium is essentially achieved in 12 minutes at 56°C. This is substantially

Table 1.3

**DICHLOROSILANE EQUILIBRIUM LIQUID
vs. VAPOR PHASE DISPROPORTIONATION AT 50-60°C**

	<u>Liquid</u>	<u>Vapor</u>
SiH ₄	11.59	16.65
H ₃ SiCl	16.10	10.40
H ₂ SiCl ₂	39.53	32.45
HSiCl ₃	32.69	40.35
SiCl ₄	0.10	0.26

longer than the 4 seconds required in the vapor phase case investigated earlier. However, the higher density helps to off-set the larger reactor volume which would be required for a given mass through-put.

The shape of the kinetic curves indicate various rate limiting resistances could be present. These preliminary data were obtained using a fixed bed height and varying the through-put and temperature. Data at other bed heights is planned to decouple any bulk flow rate effects from the intrinsic reaction rate.

The equilibrium values for 56°C obtained (Table 1.3) can be compared with the reported values for vapor phase equilibrium. The decrease in silane and trichlorosilane and increase in monochlorosilane will have a minor impact on the EPSDU process design. Assessment of this impact will be made after complete equilibrium and kinetic data are obtained next period.

Figure 1.1
CONCENTRATION of SILANE vs. RESIDENCE TIME,
DICHLOROSILANE REDISTRIBUTION

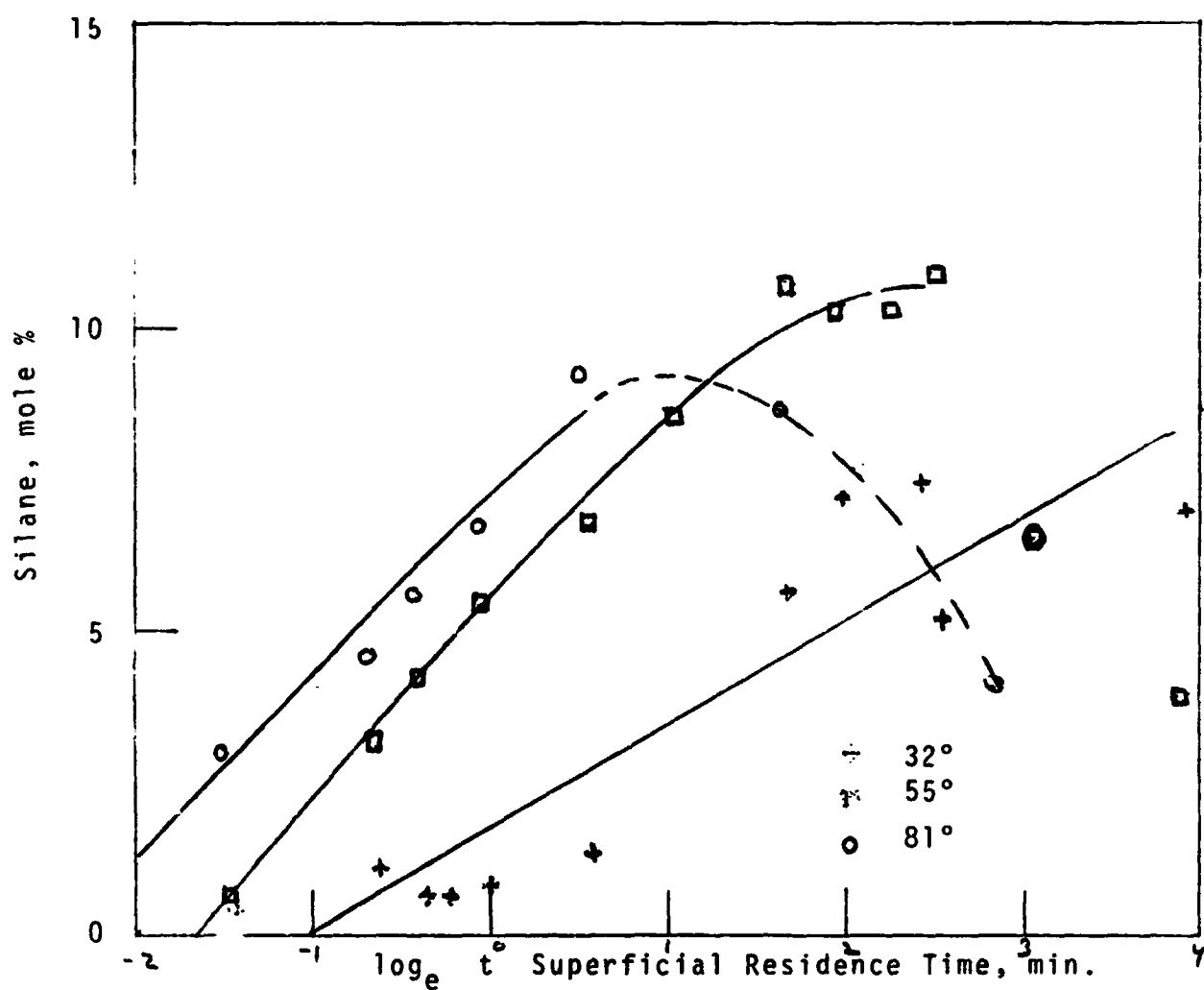


Figure 1.2
CONCENTRATION of MONOCHLOROSILANE vs. RESIDENCE TIME,
DICHLOROSILANE REDISTRIBUTION

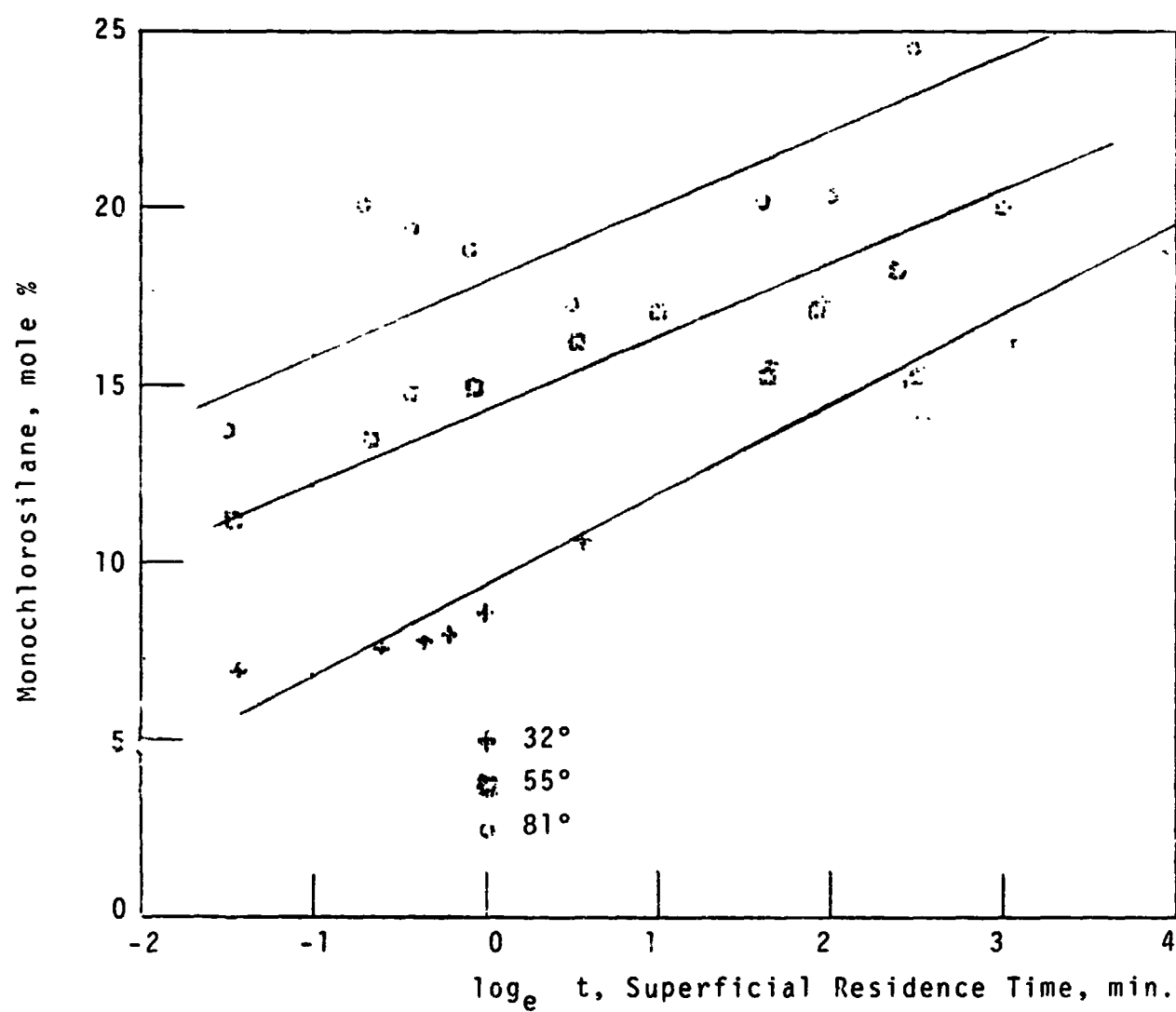


Figure 1.3
CONCENTRATION vs. RESIDENCE TIME, DICHLOROSILANE REDISTRIBUTION

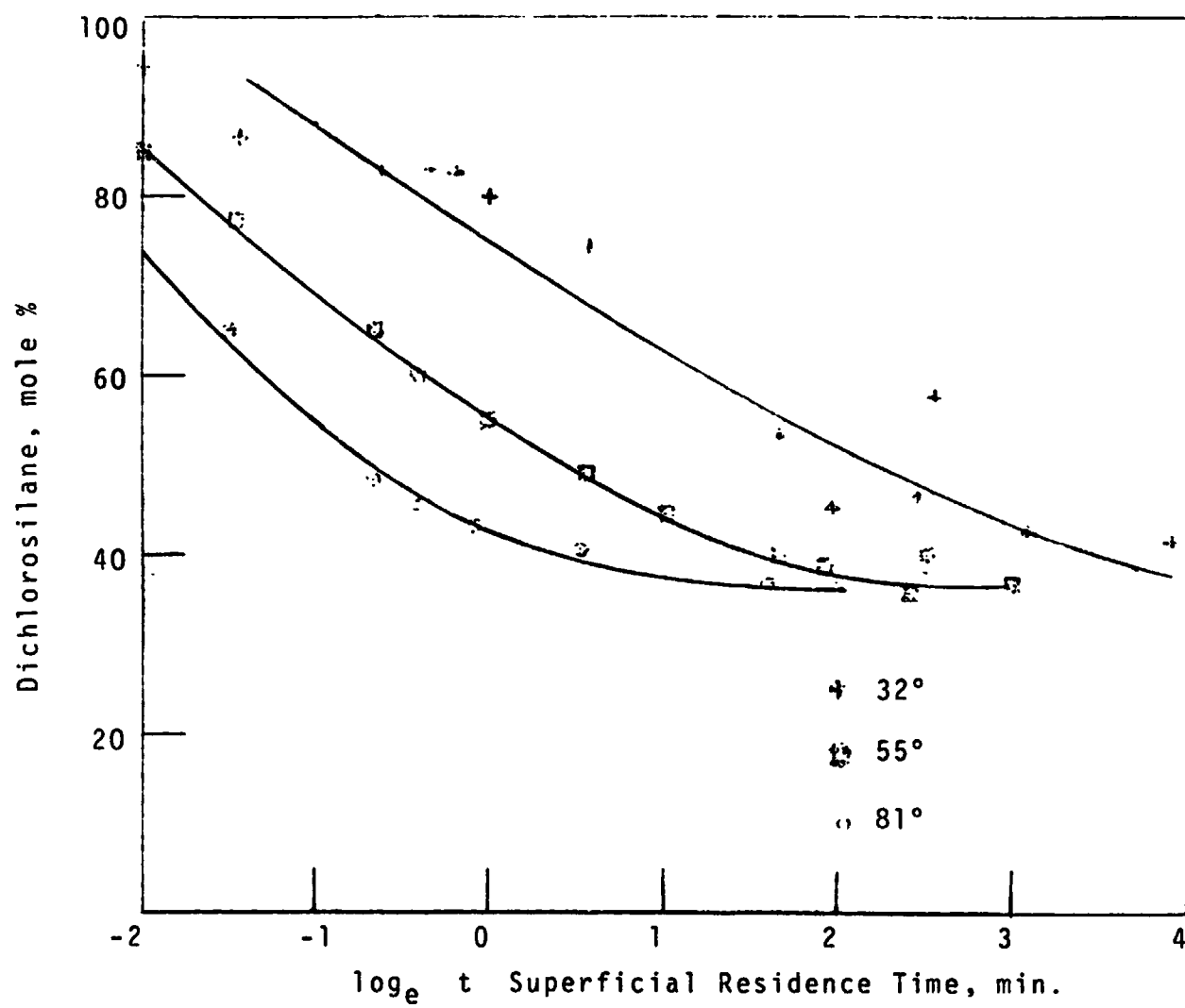
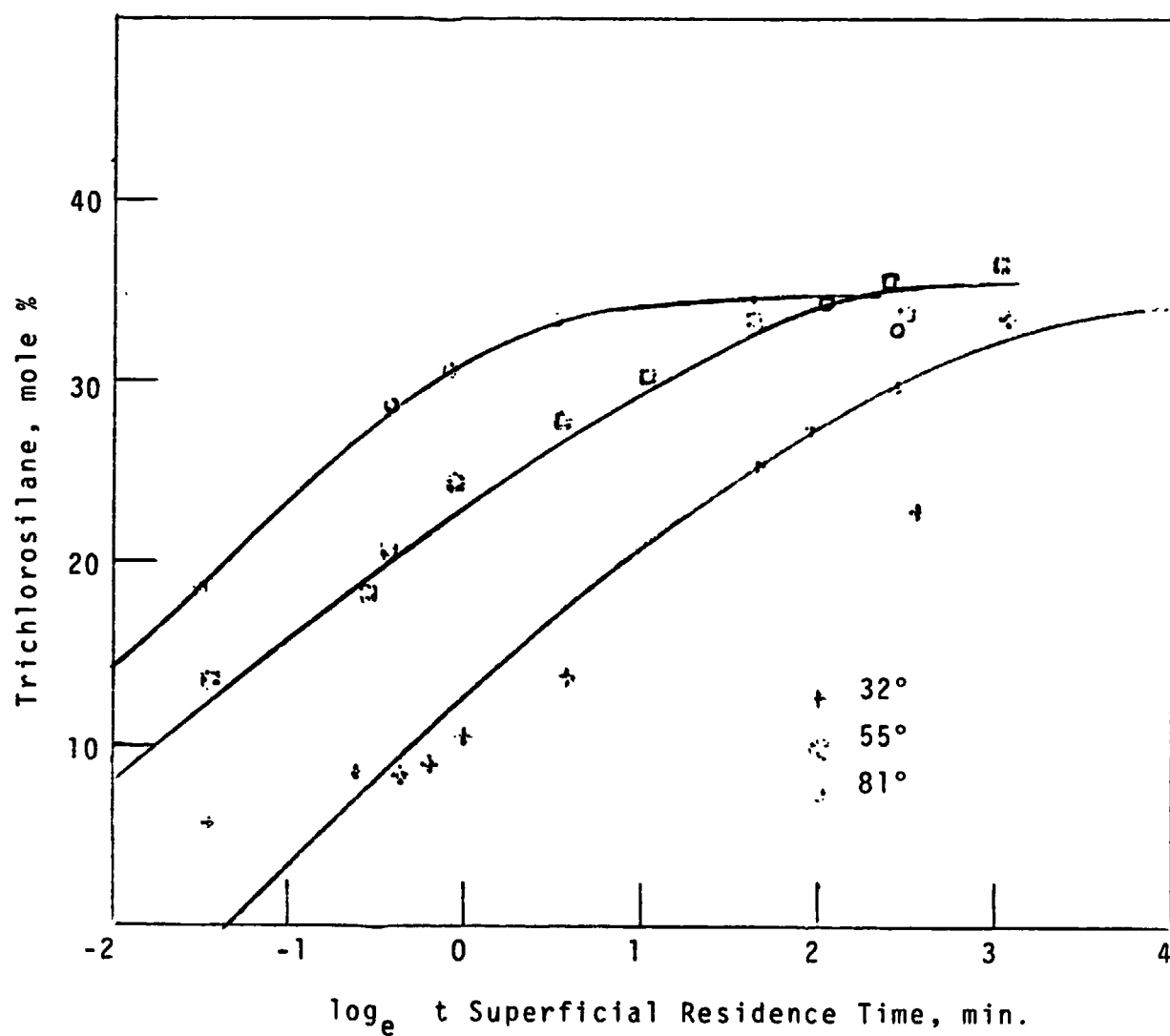


Figure 1.4
CONCENTRATION of TRICHLOROSILANE vs. RESIDENCE TIME,
DICHLOROSILANE REDISTRIBUTION



1.2.3 Hydrogenation Kinetics

The 1 inch fluid bed reactor used in earlier hydrogenation experiments was relocated and modified for operation at up to 500 psig. This will provide kinetic data at conditions planned for EPSDU.

Preliminary runs at 50 psig were made to check out the system and to gain experience. Initial low yields of HSiCl_3 resulted from channeling and poor fluidization due to a restricted distributor plate in the reactor. The feed, temperature, and pressure control systems worked well. A thermocouple has been added to monitor the reactor bed temperature directly. This unit will be used next period to determine optimum catalyst concentrations and reaction kinetics at planned EPSDU operating conditions.

A short series of experiments in a 3 inch diameter reactor were made to verify laboratory data at higher copper levels. Using 5% cement copper mixed with the metallurgical silicon and controlling the contact time at 6.9 seconds, yields of trichlorosilane of 12.7% were obtained at 50 psig pressure, Table 1.4. This compares with approximately 16% as obtained using 2% copper in the 1 inch laboratory reactor.

Table 1.4**HYDROGENATION IN 3" FLUID BED REACTOR**

Reactor Temperature	500°C	Gas Velocity	2X Minimum Fluidization
H ₂ /SiCl ₄ Mole Ratio	1.0		
Contact Time, Seconds	6.9	Copper Loading	5%

Mole %, Hydrogen Free Basis

<u>Pressure</u> <u>psig</u>	<u>H₂SiCl₂</u>	<u>HSiCl₃</u>	<u>SiCl₄</u>
50	0.99	12.77	86.24
50	1.16	12.65	86.19
100	0.38	16.72	82.90
100	1.55	18.07	80.38
100	1.71	19.19	79.10
150	3.31	16.49	80.2
150	1.51	11.25	87.24
150	2.77	14.38	82.85

The difference is likely due to fluidization quality. The gas velocity used in the laboratory study was usually below the minimum fluidization velocity of 2.1 cm/second which would result in a higher density bed. The PDU scale reactor operating at twice the minimum fluidization velocity could be expected to require longer contact to achieve the same conversion.

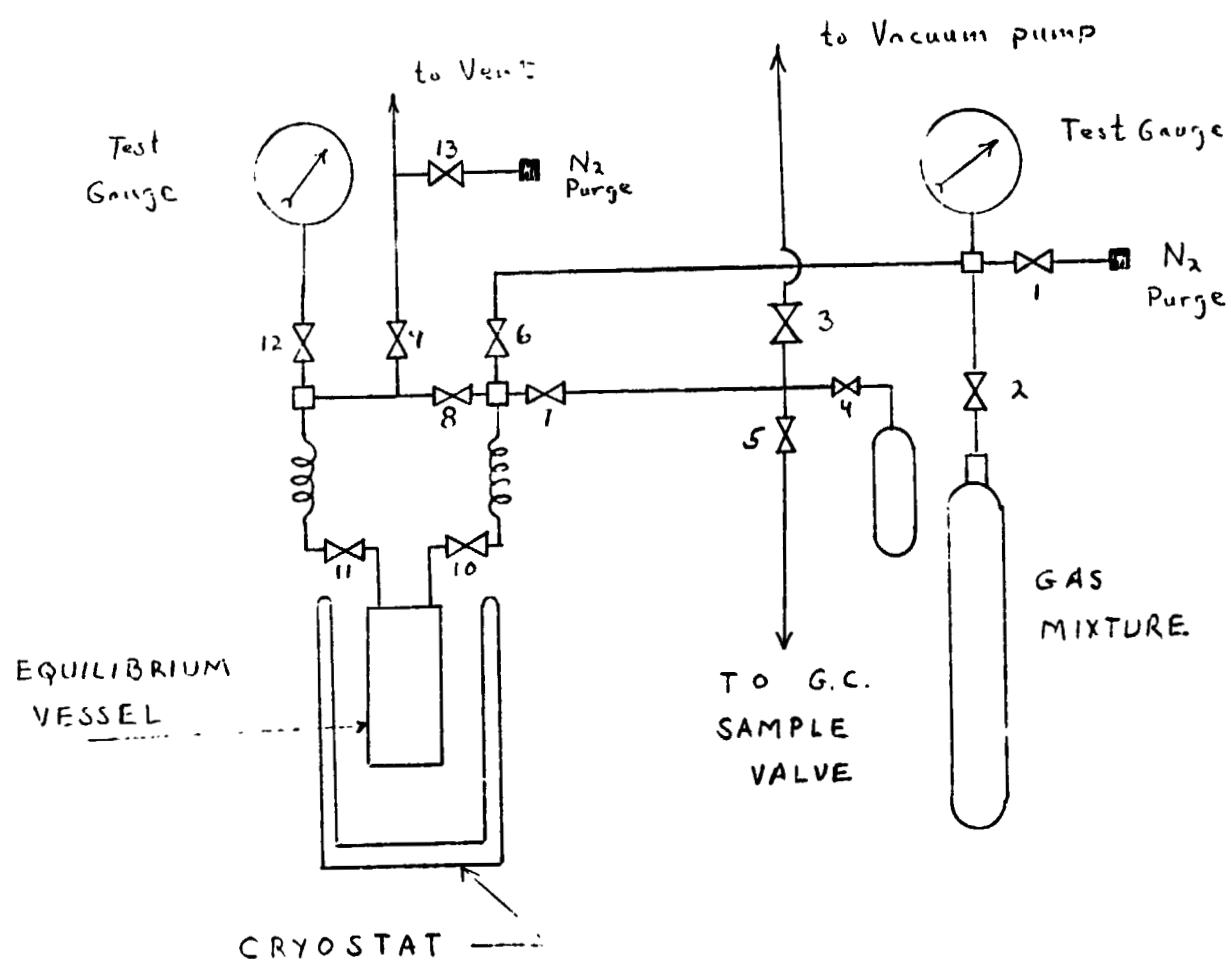
1.2.4 Silane, Phosphine, Diborane Equilibria

The final column of the proposed EPSDU process is designated to perform ultimate purification of silane by rejecting all higher boiling impurities. The closest boiling compounds to silane (bp - 112°C) which could result in electronically active species are diborane (bp - 93°C) and phosphine (bp - 82°C). The only available data on the silane-phosphine or silane-diborane system was measured at atmospheric pressure whereas the process design calls for the final column to operate at about 20 atmospheres in order to reduce refrigeration requirements. For accurate reliable design the system behavior at process conditions is needed.

An equilibrium cell and appropriate plumbing for sampling and analyzing the liquid and vapor phases was assembled and pressure tested. The basic system (Figure 1.5) consists of a 193 ml capacity equilibrium cell fitted with a small diameter dip tube and a vapor outlet. A sample of silane containing about 0.5% each of diborane, phosphine and argon can be condensed in the cell and held at the appropriate temperature by the cryostat. Small samples of the liquid and vapor phases can be withdrawn and analyzed by an integrally connected gas chromatograph.

Standard mixtures of diborane in argon, phosphine in helium and pure silane will be used to calibrate the chromatograph. These standards as well as the tertiary blend have been prepared and the chromatograph is being modified for this particular task.

Figure 1.5
SILANE VAPOR/LIQUID EQUILIBRIUM CELL



1.2.5 Materials of Construction

Either carbon steel or stainless steel appear adequate materials of construction for the disproportionation reactors. Corrosion test coupons exposed in the PDU reactors were removed for examination. The initial visual examination showed no evidence of any attack on samples of carbon or 316 stainless steel. A more detailed gravimetric and microscopic examination is underway. The exposure time was approximately 6000 hours.

For the hydrogenation reactor, the initial examination indicated Incoloy 800 is the preferred choice. Although detailed metallographic examination is still underway, the Incoloy 800 showed no visible sign of attack. All samples were coated with heavy scale deposits consisting mainly of silicon. These deposits were difficult to remove from the Incoloy and Inconel nickel based alloys but flaked off from the carbon and stainless steels. The carbon and high chrome steels also showed significant base metal attack. More detailed examination of the test coupons is in progress.

1.3 Conclusions

- Silane of extremely high purity can be the expected product from the integrated process through hydrogenation and disproportionation of chlorosilanes.
- The kinetics and equilibrium yield of dichlorosilane disproportionation in a liquid phase reactor are compatible with the latest EPSDU process design.
- Carbon steel is a preferred material of construction for the disproportionation packed bed reactors.
- Preliminary observations indicate Incoloy 800 is a preferred material of construction for the fluidized bed hydrogenation reactor.

1.4 Projected Quarterly Activities

- Hydrogenation of SiCl_4 kinetic study at EPSDU design conditions.
- Equilibrium and kinetic of HSiCl_3 and H_2SiCl_2 study at EPSDU design conditions.
- Determine vapor liquid equilibrium of diborane, phosphine and argon in Silane at high pressure.

1.5 References

- (1) Breneman, W. C., Quarterly Progress Report DOE/JPL 954334-76/3
- (2) Breneman, W. C., Farrier, E. G., Morihara, H., Quarterly Progress Report DOE/JPL 954334-78/7

2.0 SILICON PRODUCTION

2.1 Introduction

The objective of this program, which started in January, 1977, is to establish the feasibility and cost of manufacturing semi-conductor grade polycrystalline silicon through the pyrolysis of silane (SiH_4). The silane-to-silicon conversion is to be investigated in a fluid bed reactor and in a free space reactor.

In the second quarter in 1978, it was reported that a series of fluid bed reactor experiments was conducted with silane-helium gas mixtures. Under specific operating conditions, coherent silicon coatings were obtained on the seed bed particles without excessive generation of fines. In another series of experiments, silane-helium mixtures were directed both into hot empty transparent tubes and into hot transparent tubes packed with silicon particles. The products of the decomposition reactions were plate, powder, and fibers. The conditions favoring the formation of each form were studied to gain a better understanding of the mechanism of the silane pyrolysis reaction.

The free space reactor was operated for two (2) consecutive eight (8) hour long experiments, at a silicon production rate of 0.45 kg/hr, without dismantling or servicing the reactor. Loss of temperature control during the third run reduced the reactor temperature to a level that favored reactor wall formations. A single experiment was conducted to demonstrate that a high (1.8 kg/hr) silicon production rate could be obtained at a moderate Reynolds Number and reactor temperature by simultaneously increasing the gas flow and the injector orifice.

2.2 Discussion

2.2.1a Fluid Bed Reactor

The fluid bed reactor was operated continuously for 48 hours with a mixture of one percent silane in helium as the fluidizing gas. High purity-semiconductor grade silicon,* screened to -35/+60 mesh, was used as the 400 mm deep bed of seed particles. A gas flow of approximately 15 l/min was introduced into the reactor through a water-cooled porous metal distributor plate. A transparent pyrex tube having an 85 mm i.d. was used as the reactor vessel. The reactor outside wall temperature was held (in the center of the hot zone) at approximately 650°C. Operation of the fluid bed reactor during the 48-hour long run appeared to proceed without incidence. A decrease in bed height was observed and the portions of the bed that could be observed remained active. * Gas samples were collected from the exhaust gas stream at six-hour intervals; the concentration of silane present in the exhaust gas was too low to detect by infrared spectroscopic analysis. The silicon collected in the exhaust afterburner tube indicated that conversion of silane-to-silicon in the reactor was nearly complete. The experiment was terminated as scheduled.

After completion of the 48-hour long experiment, it was observed that the Pyrex reactor tube had bulged in the region between the heating elements. The drop in bed height to 350 mm was due to the increase in reactor tube diameter from 85 mm to 100 mm in this region. Examination of the seed bed revealed that a porous plug of agglomerated seed particles had formed from 80 to 150 mm above the gas distributor plate. The agglomerated plug did not extend into the region of the bulged reactor tube. Below the plug, very little seed bed plating had occurred. The majority of the plating occurred in the region of plug formation.

* Obtained from General Diode Corporation.

Above the plug, in the region where the reactor wall had bulged and the seed particles had remained fluidized, a dense, coherent coating was obtained on the seed particles (Figure 1). The coating thickness varied from 3 to 12 microns, with an average coating of 5 microns. Elutriated fines accounted for 4.8% of the total product. A mass balance indicated that the silane-to-silicon conversion efficiency was at least 90%. Higher efficiencies were indicated by infrared analysis and thermal decomposition of silane remaining in the exhaust gas stream.

The porous agglomerate formed in the 48-hour long run was sectioned and metallographically polished. The observed silane decomposition products were similar to those obtained in stagnant bed experiments and are shown in the photomicrograph in Figure 2. Both nodular and fiber-like growth occurred on the seed particles within the plug. The dense silicon plate that coated and bridged the particles, and particle-to-particle contacts before plating, were further indicators that the particles in the 48-hour long experiment were not in motion.

During the 48-hour experiment, difficulties were experienced in obtaining a stable gas flow. Consequently, a similar experiment was conducted to investigate the effect of various flow rates upon the fluidization characteristics of the bed and to determine the actual temperature of the 400 mm bed. The conditions were selected to be similar to those used in the 48-hour experiment, with the exceptions that: (1) helium was used instead of the silane-helium mixture, and (2) thermocouples were positioned inside the bed of seed particles. At a flow rate of 15 l/min, a bubbling bed was maintained and the bed temperature was $575 \pm 25^\circ\text{C}$ (reactor external wall temperature of 650°C).



ORIGINAL PAGE IS
OF POOR

Figure 2.1
CROSS-SECTION of COATED SEED PARTICLES (500X)

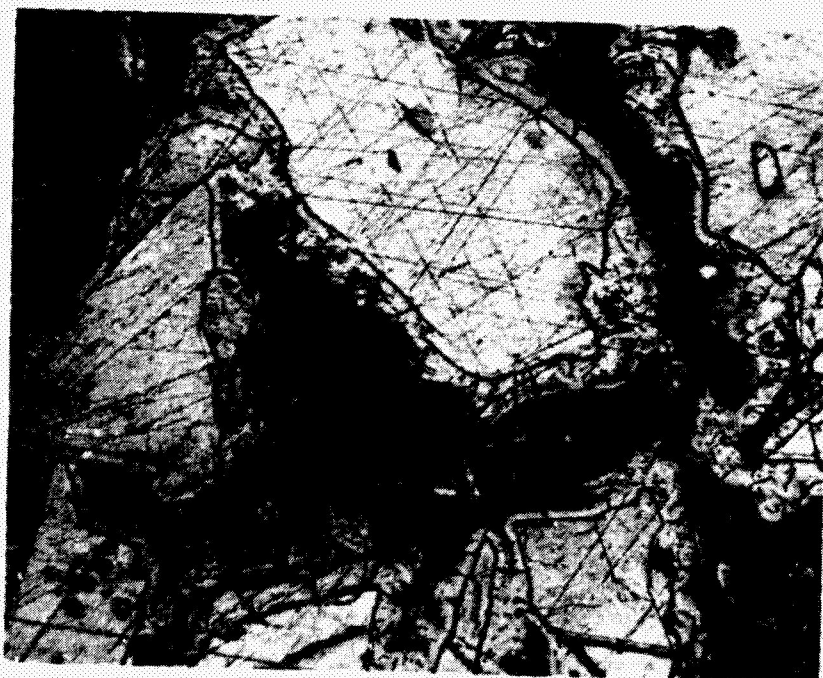


Figure 2.2
COATING on SILICON SEED PARTICLES in the AGGLOMERATED PLUG (100X)

At a flow rate of 12 l/min, the temperature gradient obtained in the bed indicated that the flow rate was insufficient to initiate bubbling in the lower region (100 or 150 mm) of the bed. The bed did not reach a temperature sufficient to pyrolyze silane until approximately 80 mm above the gas distributor plate. Therefore, no significant amount of plating occurred in this region. Above this region, the porous agglomerate formed due to lack of fluidization. The majority of the plating occurred in this region. Increased gas velocities and lower bed temperatures will eliminate the formation of porous agglomerates.

2.2.1b Free Space Reactor

The growth of silicon on the reactor wall and on the tip of the injector had to be minimized so that the free space reactor could be operated continuously or intermittently without servicing. To achieve this, several reactor modifications were made and new operating procedures were adopted for more precise control of the thermal profile of the reactor in the region near the gas injector. One reactor modification was the installation of a disc inside the quartz liner. The disc had a central hole for the gas injector and was mounted flush with the injector tip. The second modification was an injector tip extension with an orifice designed to reduce semi-solid cone formations caused by lateral diffusion and gas motion at the orifice border. Neither modification eliminated the wall buildup at low operating temperatures nor the injector cone formations at high operating temperatures. The reactor operating modifications were to (1) control the reactor wall temperature near the gas injector (instead of at the midpoint of the induction coil, which was 350 mm beneath the injector), (2) stabilize all temperatures before introducing silane, and (3) introduce silane into the reactor by slowly increasing its flow rate to the desired level. At which time, the

hydrogen flow was slowly shut down. Previously, all controls were preset for the desired silane flow and the transition from hydrogen to silane was abrupt. In a series of experiments conducted under the new operating procedure, the wall and injector deposits were reduced in thickness from a nominal 76 mm to approximately 6 mm during the four-hour runs. The thin powder deposits, with no semi-solid cones, occurred when the reactor wall (near the injector) was controlled at 700°C. Heavier deposits occurred at 750°C and 810°C. The lower temperature was selected during the consecutive series of experiments.

The free space reactor was operated for eight (8) consecutive pyrolysis experiments without dismantling or servicing of the reactor. All of the pyrolysis experiments, except one, were conducted for four (4) hours at a silicon production rate of 0.45 kg/hr. The duration of one experiment was limited to three (3) hours by the amount of silane contained in one of the cylinders. Between powder production operations, the reactor was purged with argon and cooled to room temperature. The powder was pneumatically transferred from the settling chamber to a storage hopper. Samples of powder taken from the storage hopper had free flow densities ranging from 0.12 Mg/m³ to 0.17 Mg/m³. After the first two runs of the series, the powder density range remained within 0.15 Mg/m³ and 0.17 Mg/m³ when the densities were obtained the day after the powder was produced. After remaining in the storage hopper or settling chamber from three to five days, the powder free flow density was 0.19 Mg/m³. If higher density powders are consistently obtained, the duration of the pyrolysis experiments performed in the consecutive mode of operation can be extended. The free space reactor will be operated for additional consecutive runs before it is dismantled for inspection.

2.2.1c Silicon Powder Transfer

The modified pneumatic powder discharge system for the settling chamber (attached to the underside of the free space reactor) was tested. Several 1.8 kg charges of silicon powder were transferred to a storage hopper in a matter of minutes. The powders had free flow densities ranging from 0.018 Mg/m^3 to 0.17 Mg/m^3 . In addition, the silicon powder produced in the consecutive series of experiments was pneumatically transferred. The discharge procedure was as follows. Argon was admitted to the free space reactor settling chamber assembly through the two-stage gas slides. A vacuum cleaner was attached to the discharge port of the hopper to reduce the hopper pressure. After the free space reactor assembly pressure reached five (5) psig above atmospheric, the ball valve in the powder discharge tube was opened. This valve was held open for approximately four (4) seconds. After repeating the pressurization-depressurization procedure four times, all of the powder, including the filter cake on the exhaust filter, was discharged.

2.2.1d Silicon Consolidation

Several methods were investigated for converting the free space reactor powder into a more handleable feedstock for silicon melters. One densification procedure involved vacuum sintering the free space reactor powder that was poured (not packed) into quartz crucibles. Initially, the powders had an apparent density of 0.12 Mg/m^3 and a surface area of $7.5 \text{ m}^2/\text{g}$. Powders were held at 1100°C and 1300°C for one hour. The powder sintered at 1300°C densified to 13% of the theoretical density while the surface area was reduced to $0.8 \text{ m}^2/\text{g}$. Figures 3 and 4 show scanning electron microscope (SEM) micrographs of the free space reactor powder in its as-produced condition and after the 1300°C treatment.

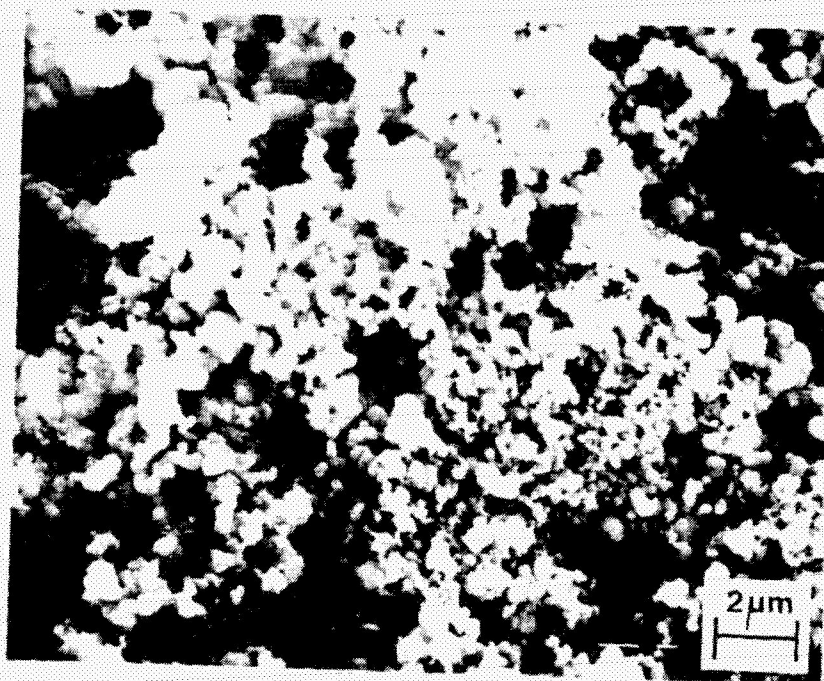


Figure 2.3
SCANNING ELECTRON MICROGRAPH
of FREE SPACE REACTOR SILICON POWDER (5,000X)

ORIGINAL PAGE IS
OF POOR QUALITY

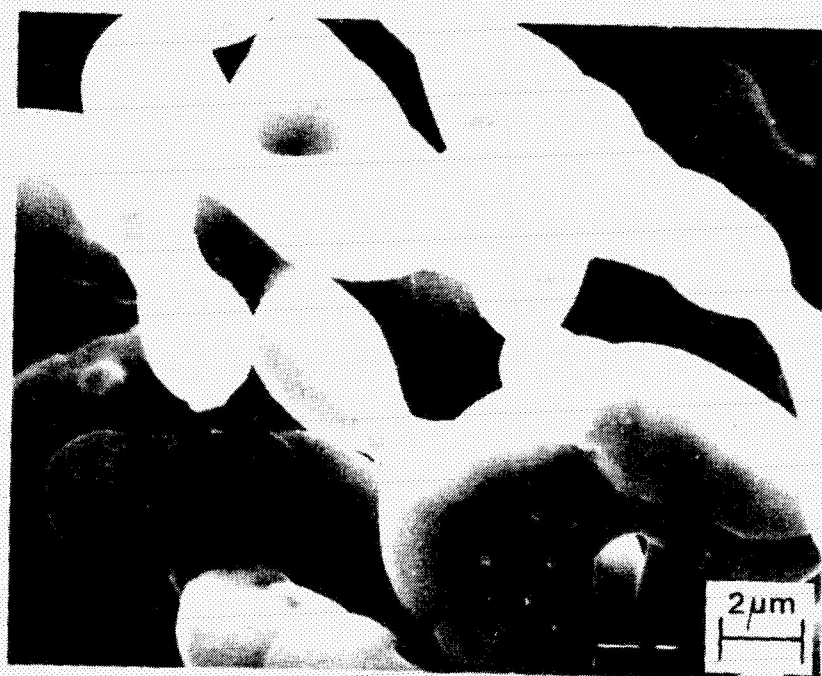


Figure 2.4
SCANNING ELECTRON MICROGRAPH
of LOOSE SILICON POWDER SINTERED UNDER VACUUM
for ONE HOUR at 1300°C (5,000X)

Loose powder sintering was an effective method for particle growth, but did not appear promising as a means of reducing the total volume of the material.

Dry pressed pellets of free space reactor powder were made without the aid of a binder. Several 12.7 mm diameter pellets were obtained at a pressure of 110 MPa. These pellets appeared to be free of delaminations. However, delaminations were apparent in the pellets after sintering at 1375°C for one hour. The apparent density of the as-pressed pellets was 47% of the theoretical density. Sintering at 1375°C did not significantly increase the apparent density of the pellets; it did increase the strength. A pelletizing process can probably be used to consolidate the free space reactor powder.

Free space reactor powder was direct rolled into flakes and sintered for one hour at 1350°C. A SEM micrograph of a flake (shown in Figure 5) revealed that the edges of the flake had undergone significant densification and particle growth or coalescence. X-ray fluorescence analysis revealed that iron, nickel, and chromium were present. These elements were probably introduced during the rolling process and may have acted as sintering promoters. Additional work on direct rolling of free space reactor powder will be necessary to minimize contamination.

2.2.1e Supporting Activities

Silicon powder that was produced in the free space reactor was analyzed for impurities by neutron activation analysis in the Livermore Laboratories in California. Through correspondence with Dr. R. Heft, it was confirmed that bromine (80 ng/g average for two samples) was the major impurity. Sodium, cobalt, and arsenic were also detected, with the sodium impurity level below 15 ng/g and cobalt and arsenic concentrations under 5 ng/g.

Since April, 1978, Dr. F. M. Galloway (staff member of the Chemical Engineering Department at Cleveland State University) has been a consultant for the free space reactor portion of the current program. Dr. Galloway's activities to date include to (1) familiarize himself with the data obtained from the operation of the free space reactor, (2) devise a model for the mechanism of heat transfer into the injected silane and the location of the reaction zone based on free jet theory and turbulent transport intensity, (3) analyze reactor and injector geometries other than the current one, (4) review conditions under which significant wall deposits or reactor plugging takes place and identify the operating parameters that would allow prediction of these occurrences, and (5) identify reactor configuration modifications that could be implemented immediately and which might lead to more efficient operation.

2.3 Conclusions

It was demonstrated that the current fluid bed reactor, with its water cooled porous metal gas distributor, was capable of pyrolyzing silane continuously for 48 hours. The reactor operating conditions that led to the formation of a porous agglomerate were identified and, with more precise control, can be avoided.

The free space reactor operating conditions were established that reduced the extent of the reactor wall deposits to a level that allowed the reactor to operate, in a consecutive mode, for a total of 31 hours to date. The current pneumatic powder transfer system was also operated successfully. The next primary task will be to operate the reactor, storage hopper, and melter as one connected unit to reduce powder exposure to atmospheric contaminants.

ORIGINAL PAGE IS
OF POOR QUALITY

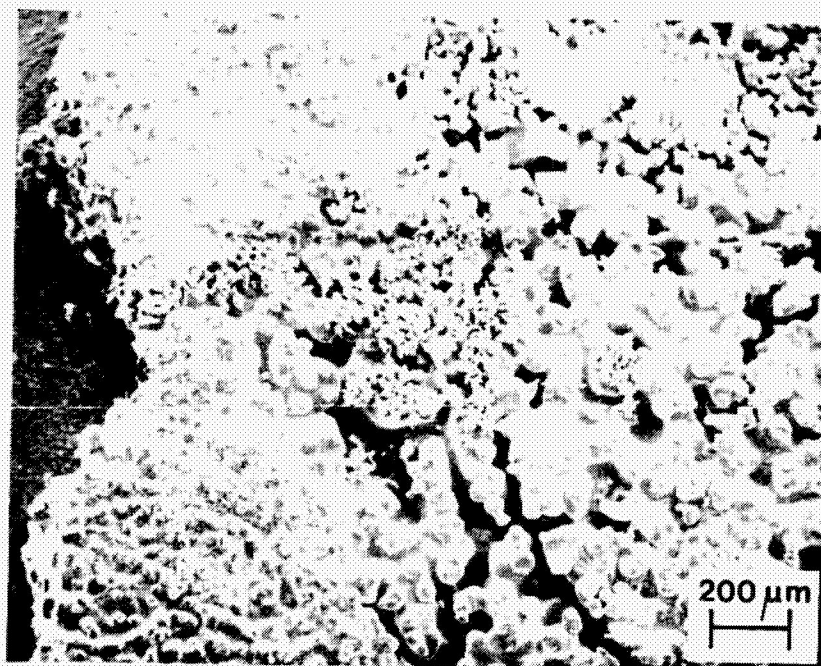


Figure 2.5
SCANNING ELECTRON MICROGRAPH
of SILICON FLAKE SINTERED UNDER VACUUM
for ONE HOUR at 1350°C (50X)

Free space reactor powder was analyzed for impurities by neutron activation analysis. The results demonstrated that the free space conversion of silane to silicon did not contaminate the silicon with the materials of construction of the reactor assembly.

Free space reactor powder pelletizing and direct rolling appear promising as alternate means of densifying the powder for enhanced handling and melter feedstock.

2.4 Projected Fourth Quarter 1978 Activities

2.4.1 Fluid Bed Reactor

A memorandum will be completed summarizing the fluid bed reactor effort.

2.4.2 Free Space Reactor

a. Conduct five (5) consecutive experiments in which silane is converted into silicon, the silicon powder is pneumatically transferred to the storage hopper with argon, and the powder is melted in a 152 mm diameter quartz crucible. All functions will be performed without dismantling or servicing the free space reactor.

b. Continue to identify critical factors that will minimize the buildup of silicon on the gas injector tip and on the reactor wall.

2.4.3 Silicon Powder Consolidation

a. Complete construction of the powder melter.

b. Establish the melting rate of free space reactor powder in the 152 mm diameter quartz crucible.

c. Continue to investigate powder pelletizing and direction rolling as means of densifying and enhancing the handling characteristics of free space reactor powder.

3.0 PROCESS DESIGN

3.1 Introduction

This program, started in October 1977, was to provide JPL with engineering and economic parameters for an experimental unit sized for 25 metric tons of silicon per year and a product-cost estimate for silicon produced on a scale of 1000 metric tons per year.

Since the experimental unit size was changed from 25 MT/Yr to 100 MT/Yr, experimental process system development unit (EPSDU), all process design work accomplished for the 25 MT/Yr unit was documented to serve as a basis for the 100 MT/Yr design. Key vapor-liquid equilibrium data has been generated and is being used to update the heat and mass balance necessary for the sizing of major equipment such as the settler and distillation columns for the EPSDU.

Other work in progress includes:

- Process design of the silane pyrolysis and melter/consolidation systems.
- Construction of a laboratory-scale waste disposal testing apparatus.
- Worksheets for the piping and instrumentation diagram.
- Generation of VLE data.

For the most part, necessary data exist to design the EPSDU with confidence except in the pyrolysis of silane and the melter

area. Melter design will receive extra attention until an acceptable design is developed.

3.2 Discussion

3.2.1 SGS Process Design for the 100 MT/Yr EPDSU

3.2.1a Heat and Mass Balance

Preparation of the heat and mass balance for the 100 MT/Yr EPDSU is in progress. Recently acquired experimental vapor-liquid equilibrium data and available open literature data for the chlorosilane family and its impurities have been successfully modeled. The programming required to make heat and mass balance and distillation calculations is operational. The method selected for vapor-liquid equilibrium non-ideality computation reproduces all experimental data well. The following equation is used:

$$k = \gamma f^L / P\phi$$

k - K-value

γ - liquid activity coefficient

f^L - liquid fugacity

P - system pressure

ϕ - vapor fugacity coefficient

For vapor-liquid equilibrium computation in the settler system for the chlorosilane components, liquid fugacity is calculated at the vapor pressure with Poynting correction from the vapor pressure to the system pressure condition. The vapor

fugacity coefficient is calculated by a two-term virial equation and the liquid-activity coefficient is calculated by the Wilson model. For the light gases (H_2 , N_2 , CO_2 , CH_4 , HCl , H_2S) Henry's constants are used for computing vapor pressure above the critical temperature, and the liquid fugacity is set equal to the vapor pressure. The liquid-activity and the vapor-fugacity coefficients have a value of about one for these materials. Ideal gas enthalpy is pressure corrected using the Redlich-Kwong equation of state down to the saturation line. At temperatures below saturation temperature, vapor enthalpy is set equal to saturated vapor enthalpy at the temperature. Below the critical temperature, liquid enthalpy is computed by subtracting the latent heat of the components from ideal gas enthalpy. Latent heat is computed by the Clausius-Clapeyron.

For the rigorous distillation simulation of the stripper, accurate vapor-liquid equilibrium data for the light gases are of prime importance. This equilibrium is computed as described above for the settler system. No pressure correction for enthalpy is made in any of the distillation simulations. Ideal gas enthalpies are used for vapor. Liquid enthalpies are determined by subtracting the component latent heat from the ideal gas enthalpy at temperatures below the critical temperature. Coefficients for the Watson correlation for computing latent heat were obtained by least squares fitting of latent heat computed by the Clausius-Clapeyron equation. Excellent fits were obtained for all chlorosilane compounds with maximum errors in the order of 1 or 2%.

For the remaining three column simulations, vapor-liquid equilibrium was also similarly calculated. The vapor fugacity coefficient for these columns was computed with the Prausnitz-Chueh correlation. Liquid fugacity was calculated at the vapor pressure with a Poynting correction. The Wilson model was used for computing the liquid activity coefficient of multi-component mixtures. Enough binary data was available in the literature and from direct measurements at a Union Carbide laboratory to confirm that this modeling method gave excellent accuracy throughout the operating range of all the columns.

An ideal vapor-liquid equilibrium value was used for computation of a heat and mass balance of the final silane polishing column No. 4. Experimental VLE data is currently being obtained for this system at our Sistersville facility; however, the data has not yet been measured and is therefore unavailable for the column computations at this time. As soon as this data becomes available it will be incorporated into the distillation computation and this heat and mass balance will be redone.

The stream catalog computer program for the 25 MT/Yr test unit was revised so as to be usable for the EPSDU application. It still has to be readied to handle impurities such as diborane, phosphine, and arsine. Correlation of impurity thermodynamic data has started. A stream catalog of all streams in the process will be generated after the heat and mass balance around the major equipment becomes available.

3.2.1b Pyrolysis System Design

Process design work on silane pyrolysis and silicon powder consolidation for the EPSDU is in progress. This section receives 21 kg/hr of high-purity silane and produces 16.4 kg/hr of polycrystalline silicon rod product. Power input requirements were estimated for both the free-space reactor and the powder melter. The reactor will be provided with three independently controlled resistance heaters of 20KW capacity each. The power required for each melter is approximately 85KW during the melting operation. When the silicon is molten, the power is cut back to its normal operating value of about 45KW.

The free-space pyrolysis reactor was scaled up from the laboratory reactor at the Parma facility on the basis of a linear relation between the reactor cross-sectional area and the throughput. This results in a reactor 2 feet in diameter by 8 feet long. Two full-size reactors are proposed for the EPSDU. The silicon powder hopper, located directly below the reactor, is approximately 4 feet in diameter by 8 feet long and is sized to hold approximately 8 hours of silicon powder inventory.

Although the melter is being designed, it is possible that commercially available equipment can be used. Initial vendor contacts were made and the results are encouraging.

The number of melters required for the EPSDU depends on the melting rate of the silicon powder and on the rate of

polycrystalline silicon rod casting. At the present time, melt rates of free-space silicon powder are not available. If the powder loading and melt rates are assumed to be similar to those of polycrystalline rods and if four 1-inch diameter rods, 4 feet in length, can be suction-cast every 15 minutes in one melter, three melters will be necessary to consolidate 16.4 kb/hr of silicon powder. A total of five melters including two spares may be required for the EPSDU. A more accurate assessment in this regard will be made as soon as the melt rate and the melter design are determined.

Several vendors were contacted to determine the most suitable method for feeding the fine silicon powder from the hopper to the melter at a controlled and measured rate. A brief test conducted with a double-screw feeder showed that steady, controlled feeding of the fine powder is possible. Vibratory and other types of feeders will also be evaluated.

A study was conducted on the materials of construction for the free-space pyrolysis system. The following materials were considered for the free-space reactor: AISI 310 SS, Monel 400, Monel K-500, Inconel 600, Incoloy 800, and Incoloy 801. These materials were evaluated based on the following criteria:

- Strength at operating temperatures
- Compatibility with environment under operating conditions
- Possible contamination of product via diffusion,

vaporization, or erosion of materials of construction

- Cost

Incoloy 800 appears to be the most suited for the pyrolysis reactor application. Incoloy 801 gives better strength and stability at high temperature; however, it is available only in sheets, strips, rods, and bars. Because of this, the fabrication cost of an Incoloy 801 vessel should be more expensive. Other metal parts such as the hopper should be made of 316 SS.

3.2.1c Piping and Instrumentation Worksheets

Piping and Instrumentation worksheets have been prepared for all sections except the waste treatment and the pyrolysis sections. The P&I worksheets show all piping, electrical and pneumatic lines, valves, and control instruments. These worksheets are used by the instrumentation engineers to design the total control system to generate P&I diagrams. Detailed engineering work has been in progress for over a month. The optimum method of instrumentation and control and specific hardware for each control loop are being determined.

3.2.1d Waste Disposal Testing

Disposal of waste sludge containing metal chlorides in chlorosilanes from the EPSDU has to be made in a manner that conforms with environmental regulations. Information is being gathered concerning waste treatment of process wastes by chemical

oxidation with lime and thermal oxidation in a combustion chamber. A small bench-scale apparatus has been designed for testing the feasibility of sludge treatment by acid hydrolysis and lime neutralization. Figure 3.1 shows the system schematic diagram. Fabrication of a plastic pipe reactor and associated equipment has been started. Silicon tetrachloride will be used in place of sludge for preliminary experiments since STC is the main liquid component of the waste stream. Later, the apparatus will be used to treat actual settler sludge.

Gaseous wastes will be treated by thermal oxidation. Information on such disposal from both the UCC Sistersville and Keasbey plants indicates that a higher degree of combustion product treatment will be required than was initially intended. The silica formed on combustion of chlorosilane has a fine particle size and is, therefore, difficult to capture.

3.2.1e Adsorption System Design

Design of a temperature-swing adsorption purification system was completed. Figure 3.2 shows the system schematic diagram. It is a redundant silane purification feature placed downstream of the silane distillation column. The adsorption trap, consisting of high-purity silica gel, is sized to adsorb all impurities in the event of an upset and maintain the desired purity level of less than one part per billion.

This adsorption system was eliminated from the EPSDU design because:

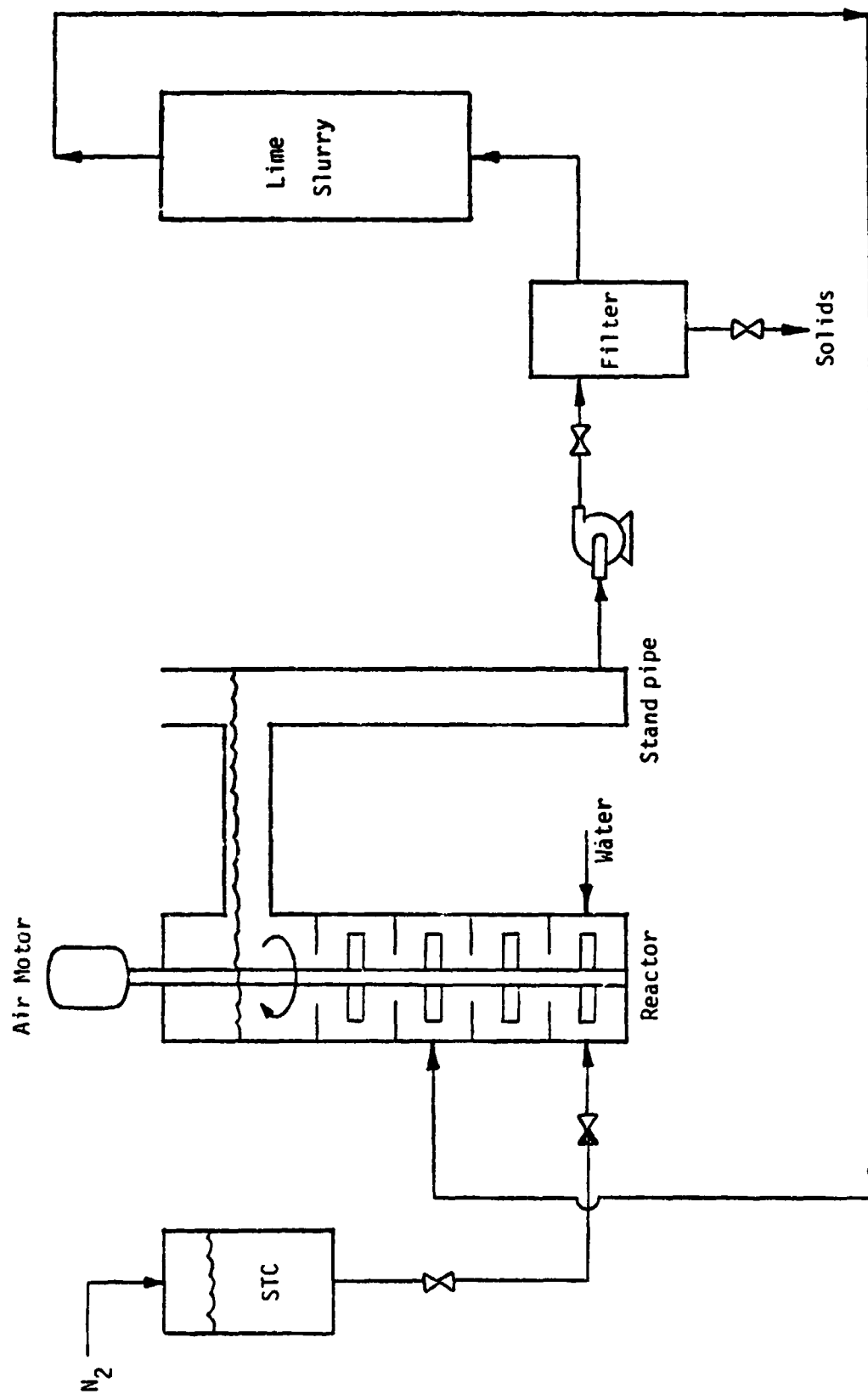
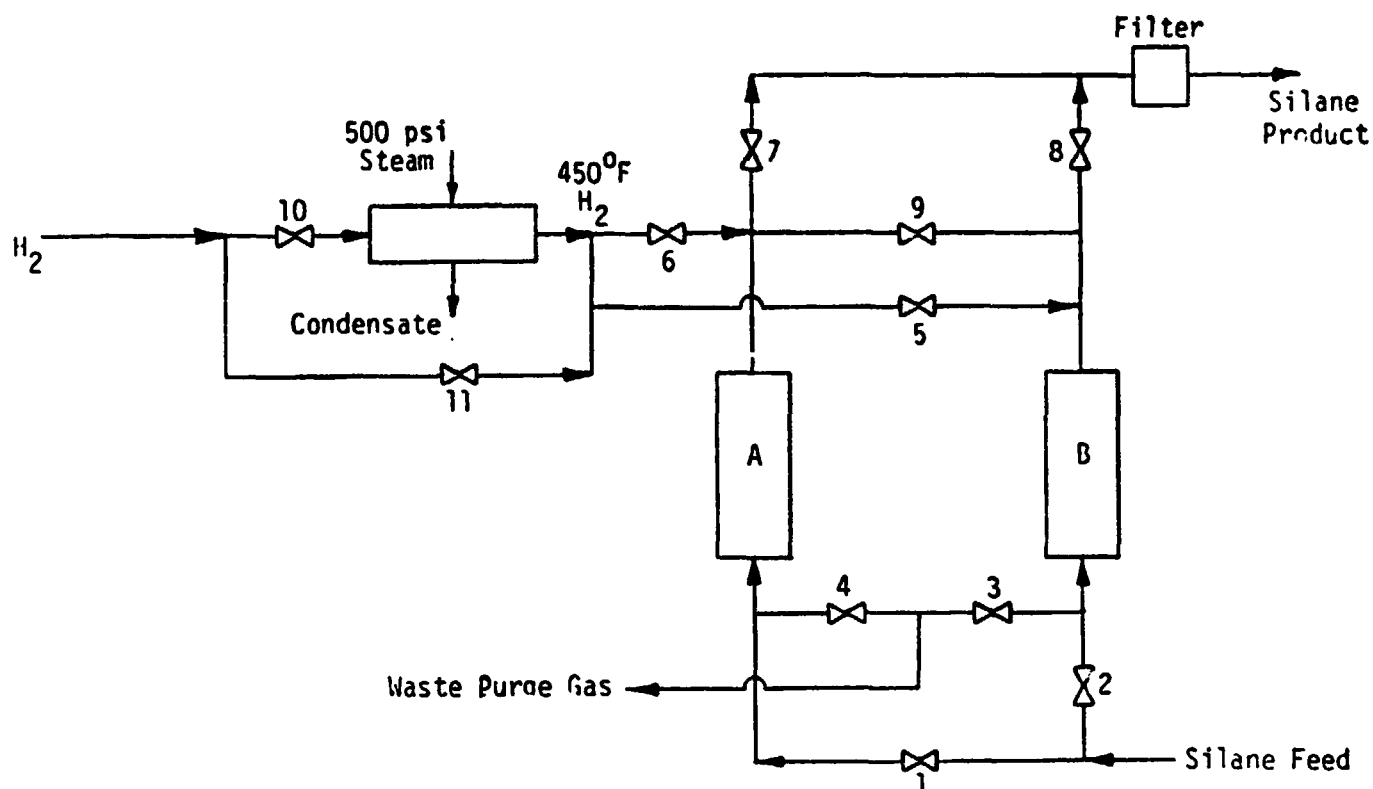


Figure 3.1
FLOWSHEET of APPARATUS for HYDROLYSIS and LIME
NEUTRALIZATION of SILICON TETRACHLORIDE



Bed Size: 8" pipe, 5½ feet long

Bed Weight: 83 lb silica gel

Bed A on regeneration, 8 hr cycle

Bed B on adsorption

<u>Time - Hr</u>		<u>Valves Open</u>
0 - 0.2	Bed A depressurizing	2, 4, 8
0.2 - 2.9	Bed A heating	2, 4, 6, 8, 10
2.9 - 6.6	Bed A cooling	2, 4, 6, 8, 11
6.6 - 7.6	Bed A silane purge	2, 4, 9
7.6 - 8	Bed A repressurization	2, 9

Figure 3.2
ADSORPTION SYSTEM FLOWSHEET

- . the distillation system is designed to remove all impurities to specification levels; therefore, the adsorbent system is redundant
- . valving and reactivation equipment added substantial complication and cost to the plant
- . contaminant in the adsorbent matrix, at high-silane purity, has a higher probability of adding contaminants than removing them

3.2.2 Process Design Data and Modeling

3.2.2a Data Acquisition

Certain process design data are being acquired in order to be able to design the EPSDU accurately. The binary vapor-liquid equilibrium for H_2SiCl_2 - HSiCl_3 at 100, 200, and 300 psia was completed. Gas solubility data for N_2 , CH_4 , and CO_2 in H_2SiCl_2 and HSiCl_3 were also obtained at 30° and 60°C . These tests results were reported in the April-June Quarterly Progress Report.

Most of the remaining experimental data were obtained during the current reporting period. The first experiments were to determine the vapor pressures of H_2SiCl_2 and HSiCl_3 . Table 3.1 contains boiling points of the pure materials at 100, 200, and 300 psia. An Antoine equation fit to these points is also given. It must be noted that this Antoine equation should

Table 3.1
PURE COMPONENT VAPOR PRESSURE

Dichlorosilane

<u>T(°C)</u>	<u>P(psia)</u>
71.8	102.0
71.4	102.0
102.6	202.0
102.7	202.0
123.6	299.4
123.6	299.4

Antoine Eq. $\log_{10}P = A-B/(T+C)$
 A= 5.40919
 B= 1113.28
 C= 255.979

Trichlorosilane

<u>T(°C)</u>	<u>P(psia)</u>
102.4	101.0
102.7	102.0
137.0	201.0
136.9	201.0
159.7	299.4
159.9	299.4

Antoine Eq. $\log_{10}P = A-B/(T+C)$
 A= 5.70513
 B= 1459.89
 C= 292.236

be used only for applying experimental data on these particular sample in this particular pressure-temperature range. Process simulations should use an extended range Antoine equation valid for the entire liquid temperature range.

Gas solubility data for N_2 , CH_4 , CO_2 , and HCl in H_2SiCl_2 , $HSiCl_3$, and $SiCl_4$ were measured by a gravimetric method^(3.1) at 30° and $60^\circ C$. The data were obtained by weighing an amount of degassed liquid added to an evacuated Hoke bomb, adding a precisely weighed sample of gas, and then measuring the final pressure after shaking the bomb and allowing it to stand in a constant temperature bath. The experimental data, in terms defined in Table 3.2, are presented in Tables 3.3 to 3.5.

Silane, diborane, phosphine vapor-liquid equilibrium experiments remain to be conducted. The data will be obtained at our Sistersville facility.

3.2.2b Chemical Equilibrium and Heats of Formation

A departmental engineering memorandum titled "Chemical Equilibrium and Heat of Formation, Chlorosilane Family" was written.^(3.2) It contains 1) five reactions which define equilibrium distribution of chlorosilanes in the hydrogenation reactor; 2) an equation which defines equilibrium constants for the five reactions; 3) heats of reaction, correlation constants, and equilibrium constants for each of the five

Table 3.2

DEFINITION OF TERMS IN EXPERIMENTAL RAW DATA TABLES

T(°C)	= Celsius temperature
P(atm)	= Total pressure at equilibrium
V(cc)	= Total volume at Hoke sample bomb, measured in separate calibration experiment
MG(g)	= Total mass of gas (solute) added to sample bomb
ML(g)	= Total mass of liquid (solvent) added to sample bomb

- - - - -

X2	= Mole fraction of gas dissolved in liquid phase. <u>NOTE: This is a calculated quantity, not an experimental measurement.</u>
----	--

Table 3.3

EXPERIMENTAL DATA N_2 , CH_4 , CO_2 , and HCl IN DICHLOROSILANE

T(°C)	P(atm)	V(cc)	MG(g)	ML(g)	X2	
30.00	18.311	337.750	3.331	253.014	0.016478	N_2
30.00	18.253	337.750	3.493	228.324	0.014822	
30.00	18.321	337.750	3.299	250.972	0.015674	
60.00	22.268	337.750	3.331	253.014	0.021738	
60.00	22.064	337.750	3.493	228.324	0.020794	
60.00	22.217	337.750	3.299	250.972	0.021073	
30.00	18.168	337.750	3.779	245.222	0.060637	CH_4
30.00	17.692	337.750	3.573	218.017	0.056987	
60.00	23.102	337.750	3.779	245.222	0.064229	
60.00	22.404	337.750	3.573	218.017	0.060760	
30.00	7.281	337.750	9.184	265.077	0.066832	CO_2
30.00	7.417	337.750	8.424	223.479	0.068232	
60.00	11.942	337.750	9.184	265.077	0.066950	
60.00	12.061	337.750	8.424	223.479	0.067628	
30.00	6.941	337.750	9.526	257.428	0.086335	HCl
30.00	6.907	360.015	9.495	254.011	0.085507	
60.00	11.568	337.750	9.526	257.428	0.086274	
60.00	11.568	360.015	9.495	254.011	0.085034	

Table 3.4

EXPERIMENTAL DATA N_2 , CH_4 , CO_2 , and HCl IN TRICHLOROSILANE

T(°C)	P(atm)	V(cc)	MG(g)	ML(g)	X2	
30.00	21.111	337.750	4.101	282.575	0.022094	N_2
30.00	21.792	337.750	4.284	273.425	0.021496	
60.00	24.194	337.750	4.101	282.575	0.026498	
60.00	24.874	337.750	4.284	273.425	0.026278	
30.00	21.860	337.750	4.583	259.474	0.081187	CH_4
30.00	21.792	337.750	4.535	255.905	0.079914	
60.00	26.130	337.750	4.583	259.474	0.083307	
60.00	25.993	337.750	4.535	255.905	0.082124	
30.00	10.547	337.750	15.279	276.295	0.128983	CO_2
30.00	7.145	337.750	8.780	273.358	0.076992	
60.00	15.445	337.750	15.279	276.295	0.126638	
60.00	10.479	337.750	8.780	273.358	0.075777	
30.00	7.315	337.750	8.779	268.113	0.094962	HCl
30.00	7.315	360.015	9.357	271.300	0.098313	
60.00	10.649	337.750	8.779	268.113	0.093754	
60.00	10.785	360.015	9.357	271.300	0.096486	

Table 3.5

EXPERIMENTAL DATA N_2 , CH_4 , CO_2 , and HCl IN TETRACHLOROSILANE

T(°C)	P(atm)	V(cc)	MG(g)	MG(g)	X?	
30.00	20.941	337.750	4.176	316.632	0.024851	N_2
30.00	20.073	360.015	4.329	318.343	0.021036	
60.00	24.054	337.750	4.176	316.632	0.029859	
60.00	22.489	360.015	4.329	318.343	0.026298	
30.00	21.792	337.750	4.543	311.784	0.087788	CH_4
30.00	20.073	360.015	4.543	307.035	0.083263	
60.00	25.585	337.750	4.543	311.784	0.090645	
60.00	22.612	360.015	4.543	307.035	0.085507	
30.00	7.179	337.750	8.951	307.484	0.085539	CO_2
30.00	6.907	360.015	8.784	311.385	0.080963	
60.00	10.003	337.750	8.951	307.484	0.084071	
60.00	9.560	360.015	8.784	311.385	0.079283	
30.00	6.662	337.750	7.630	307.159	0.089344	HCl
30.00	7.247	360.015	8.444	305.158	0.095670	
60.00	9.322	337.750	7.630	307.159	0.088000	
60.00	10.071	360.015	8.444	305.158	0.093631	

reactions; and 4) the best heats of formation values available for the chlorosilane family including silane, silicon tetrachloride, and hydrogen chloride.

3.2.2c Redistribution Rate Constants

A computer program was written which determines rate constants for the three simultaneous redistribution reactions. An attempt to use the program to compute second-order rate constants for a set of vapor-phase dichlorosilane data was not successful. A deficiency in the measurement precision of silicon tetrachloride at low concentration levels is believed to be responsible for the convergence failure. Data smoothing should correct this difficulty.

3.2.3 Other Activities

3.2.3a Engineering Practices Package

An engineering design standards package is being prepared based on Sistersville plant experience and sound engineering judgment. The package will identify materials and types of piping and valving suitable for various process conditions and will also contain maintenance and safety practices commonly used in a unit of this type.

The package will be expanded gradually as the design progresses and will become comprehensive design standards that

will be valuable for a similar unit of any size.

3.2.3b Product Sample Analysis

Discussions on analytical requirements of the EPSDU are being conducted with in-house consultants. These discussions have been particularly valuable in setting limitations on state-of-the-art silane analysis. We plan to provide as complete an analytical capability as possible so that timely confirmation of design performance can be made. We believe that a rapid component analysis of process streams is desirable to assess facility performance.

3.2.3c Equipment Vendor Identification

Various vendors have been identified for possible sources for a pneumatic powder transport system and a screw-type powder metering and feeding system from the free-space reactor to the melter. A vendor has been contacted that will allow us to use his equipment to test the flow characteristics of silicon powder. Free-space silicon powder has been received and will be dried before testing. Vendor contacts are being made to obtain budget prices for equipment used in the EPSDU. Budget prices for diaphragm compressors have been obtained.

3.2.3d Process System Valving and Piping

A study has been started to select the types and requirements of process system valving and piping. It appears that lightweight valves and PVC-coated steel tubes seem feasible for

most modest temperature applications. The study will include material selection.

3.3 Conclusions

Process design for the 100 MT/Yr EPSDU is well underway. With the new experimental thermodynamic data, the programming required to make heat and mass balance and distillation calculations is operational. This enables complete characterization of the process streams and more precise specifications for major equipment.

With the use of the small bench-scale waste disposal testing apparatus, disposal of waste sludge from the EPSDU can be made in a manner that conforms with environmental regulations. The apparatus is under construction.

Process design work on silane pyrolysis and silicon powder consolidation for the EPSDU is in progress. The free-space reactor was scaled up from the process development unit (PDU) being tested at our Parma facility. The silicon powder melter system is being designed based on the PDU design, but commercially available melters are also under investigation. Two full-size free-space reactors and five melters, including two spares, will probably be installed in the EPSDU to process the available silane on a continuous basis.

Materials of construction for the free-space pyrolysis system has been determined. Incoloy 800 appears to be the most

suited for the pyrolysis reactor application. Other metal parts such as the hopper should be made of 316 SS.

3.4 Projected Quarterly Activities

3.4.1 Heat and Mass Ballance

A mass balance of all major streams including trace components will be made. A heat balance will then be completed for all major pieces of equipment for the 100 MT/Yr EPSDU.

3.4.2 PFD and Stream Catalog

The process flow diagram for the 100 MT/Yr EPSDU will be completed and issued. The stream catalog of all streams will be completed. The impurity mass balance will be included in the stream catalog.

3.4.3 Functional Equipment Specifications

All functional equipment specifications for the 100 MT/Yr EPSDU will be completed.

3.4.4 Key Equipment Design

Key equipment design will be started in the next quarter.

3.4.5 Waste Disposal Testing

Waste disposal testing will proceed using the chemical oxidation with lime method and the thermal oxidation method. A decision will be made as to which one is best suited in our process.

3.4.6 P&I Diagram

The first issue of the P&I diagrams will be completed by the end of the quarter.

3.4.7 Major Equipment Costing

Costing of major equipment for the 100 MT/Yr EPSDU will be substantially completed. Costing of the 1000 MT/Yr plant will be in progress.

3.4.8 Pyrolysis System Design

The process and functional design work on the pyrolysis reactor and silicon hopper will be completed. Conceptual design of the melter and suction-casting equipment will be started. Vendor contacts for melting hardware will be pursued.

3.5 References

- 3.1 J. D. Olson, J. Chem. Eng. Data 22 (1977), 326.
- 3.2 R. A. Beddome, "Chemical Equilibrium and Heats of Formation, Chlorosilane Family", Engineering Memorandum NO. 6266 (SGS-20), Union Carbide Corporation, Linde Division, Tonawanda, New York, June 28, 1978.

4.0 FLUID-BED PYROLYSIS R&D

4.1 Introduction

The purpose of this program is to explore the feasibility of using electrical capacitive heating to control the fluidized silicon-bed temperature during the heterogeneous decomposition of silane and to further explore the behavior of a fluid bed. These basic studies will form part of the information necessary to assess technical feasibility of the fluid-bed pyrolysis of silane.

A high-capacitive power source was obtained to see if a silicon bed can be heated to 900°C capacitively. Tests were delayed due to a transformer failure.

Both 2- and 6-inch diameter cold beds are used to study the basic fluid-bed behavior of silicon particles. Scaling laws indicate that lead particles fluidized by room-temperature helium can model 900°C silicon particles fluidized by a silane-hydrogen mixture.

Fluid-bed pyrolysis requires replenishment of seed particles. Fines produced in a fluid-bed may serve this purpose. Basic long-duration tests are conducted to determine attrition rates with time, temperature, U/U_{mf} , particle size, and silicon purity.

4.2 Discussion

4.2.1 Theoretical Investigations

4.2.1a Fluid-Bed Scaling Laws

For the fluid-bed modeling with inert gas, the scaling laws suggested by Dr. T. Fitzgerald of Oregon State University^(4.1) are being used. According to the laws, the following four dimensionless parameters of the actual and the model systems must match:

$$\frac{gL}{U^2}, \frac{L}{d}, \frac{\rho_g}{\rho_s}, \frac{d\rho_g}{\mu}$$

where g = gravitational acceleration

L = bed dimension (bed diameter)

d = bed particle diameter

ρ_g = gas density

ρ_s = particle density

μ = gas viscosity

U = fluid velocity

The original derivation of the laws reportedly is from a continuous model for a fluid-bed, but they can also be derived by assuming constant proportionality of the inertial, gravitational, and viscous forces on the particles. The laws can also be written as:

$$\rho_{sm} = \rho_{sa} \left(\frac{\rho_{gm}}{\rho_{ga}} \right)$$

$$U_m = U_a \left(\frac{\rho_{ga} \mu_m}{\rho_{gm} \mu_a} \right)^{1/3}$$

$$d_m = d_a \left(\frac{\rho_{ga} \mu_m}{\rho_{sm} \mu_a} \right)^{2/3}$$

$$L_m = L_a \left(\frac{\rho_{ga} \mu_m}{\rho_{gm} \mu_a} \right)^{2/3}$$

Subscript "m" indicates the model system and "a" indicates the actual system.

The actual system to be modeled is a 900K silicon particle bed fluidized by a mixture of hydrogen and silane. If the fluidizing gas (mixture) is mostly hydrogen, the corresponding cold model system is lead particles fluidized by helium with a 3:1 reduction in size. This will be the initial model for testing. It has also been suggested that we model cases in which the fluidizing gas contains a significant amount of silane in hydrogen. These cases will be modeled; however, the model cannot exactly simulate the true system. The reason is that in the actual system silane pyrolysis in the bed causes a silane concentration gradient along the vertical axis of the bed which the model does not have. Furthermore, the concentration gradient is unknown and is a function of the pyrolysis efficiency and of the degree of back mixing. The benefit of using a tapered fluid-bed because of the increase in flow due to silane decomposition has often been questioned. Simple calculations indicate that U/U_{mf} may go up only

20% from the bottom to the top of the bed. The increase is probably not monotonic. For any inlet concentration of silane up to 50%, U/U_{mf} first increases as silane is decomposed, but the increase is offset somewhat by an increase in U_{mf} due to a decrease in gas viscosity. Consequently, it appears that a bed taper is not necessary for the cases currently of interest. A tapered bed may be more appropriate when the silane concentration is very high and/or when the bed is deep.

4.2.1b Fixed-Bed Pyrolysis Modeling

For a complete understanding of fluid-bed pyrolysis, fixed-bed experiments are valuable since the operating parameters can be controlled much easier in a fixed-bed than in a fluid-bed. Caution must be exercised in interpreting fixed-bed data recognizing the differences in fluid-and fixed-bed behaviors. We believe that fixed bed experiments are of value to determine the following:

- . Critical concentrations
- . Plating rates
- . Effect of pressure on critical concentrations and plating rates
- . Morphology of the plated material

An analytical model for fixed-bed pyrolysis was generated and underwent debugging employing limiting cases of known solutions. Calculations are underway to determine operational

limits of the fixed bed. Preliminary indications are that up to 20% mole fraction of silane can be fed at the bed temperature of 900K. The governing equation for the analysis is given below:

The general equation for heat flow in the packed bed is:

$$\begin{aligned} & \rho_{\text{SiH}_4} (1-\epsilon) C_p^{\text{Si}} \frac{\partial T}{\partial t} \\ = & \nabla \cdot (k_e \nabla T) - \frac{\partial}{\partial x} (\rho_{\text{SiH}_4} U h_{\text{SiH}_4} + \rho_{\text{H}_2} U h_{\text{H}_2}) \\ & + h_{\text{Si}} \frac{\partial}{\partial x} (\rho_{\text{SiH}_4} U \frac{m_{\text{Si}}}{m_{\text{SiH}_4}}) \end{aligned}$$

ϵ = bed voidage

ρ_{Si} = mass density of silicon

ρ_{SiH_4} = mass density of silane

ρ_{H_2} = mass density of hydrogen

C_p^{Si} = heat capacity of silicon

h_{H_2} = enthalpy of hydrogen (per unit weight)

h_{SiH_4} = enthalpy of silane (per unit weight)

h_{Si} = enthalpy of silicon (per unit weight)

U = gas velocity

T = temperature

k_e = effective thermal conductivity

m_{Si} = molecular weight of silicon

m_{SiH_4} = molecular weight of silane

In writing this equation, it is assumed that the gas and solid are at the same temperature at any point in space. This is a good approximation, as can be seen by comparing the thermal relaxation time, τ_t , with the amount of time required for the gas to move one particle diameter, τ_d .

$$\tau_t = \frac{d_p^2}{\alpha}$$

$$= \frac{(200 \times 10^{-6} \text{ m})^2}{(5 \times 10^{-4} \frac{\text{m}^2}{\text{s}})} = 8 \times 10^{-5} \text{ s}$$

$$\tau_d = \frac{d_p}{U}$$

$$= \frac{(200 \times 10^{-6} \text{ m})}{(10^{-2} \text{ m/s})} = 2 \times 10^{-2}$$

d_p = particle diameter

α = thermal diffusivity

$$\tau_d \ll \tau_t$$

This implies that the gas temperature will relax to the solid temperature before the gas moves a fraction of a particle diameter, so no distinction need be made between the two.

The change in composition is governed by:

$$\frac{\partial}{\partial x} (\rho \text{SiH}_4 U) = r a$$

a = surface area/unit volume

r = reaction rate

This equation, the equation of state for an ideal gas, and the stoichiometry of the reaction determine the composition of the gas and the velocity at any point in the bed, if these are known at the inlet. The time rates of change are slow for this to be a reasonable approximation. The reaction rate is taken from the epitaxial rate data discussed in the fixed bed experiments section.

The inlet conditions of the gas (composition, temperature, and flow rate) and the wall temperature are inputs to the model. The problem is axisymmetric. The solution is achieved by replacing the governing differential equation by finite difference equations, and integrating forward in time. This is done in the same manner as for transient two-dimensional heat transfer problems. There is no fundamental problem in the numerical algorithm, but there are upper limits on step sizes in space and time for stability and accuracy.

4.2.2 Experimental Work

4.2.2a High-Temperature Fluid-Bed

The apparatus for demonstrating high-frequency electrical heating to high temperature was shown in Figure 4.4 of the April-June Quarterly Progress Report.^(4.2) The system check-out was made by heating the bed to 300°C at the inlet gas temperature of 200°C. The reactor then was heated to 500°C and some pressure drop vs flow rate measurements were made. However, the experiment had to be terminated due to the faulty transformer in the high-power equipment. The transformer will be replaced by the manufacturer by early October.

4.2.2b Cold Modeling Experiments

Basic fluid-bed behavior study is conducted with 2-inch and 6-inch diameter cold beds made of glass cylinders. First series of experiments were conducted with the 2-inch diameter bed. Lead and silicon particles were fluidized with air and helium. The scaling laws described in Section 4.2.1a show that the fluidization behavior should be near identical between the lead particles fluidized with helium at room temperature in a 2-inch diameter column and silicon particles three times the size of the lead particles fluidized with hydrogen at 900°K in a 6-inch diameter column. Results of two scale-model tests with +35 mesh lead and -35/+60 mesh lead are shown in Figures 4.1 and 4.2. These lead particle sizes correspond to silicon particles in a

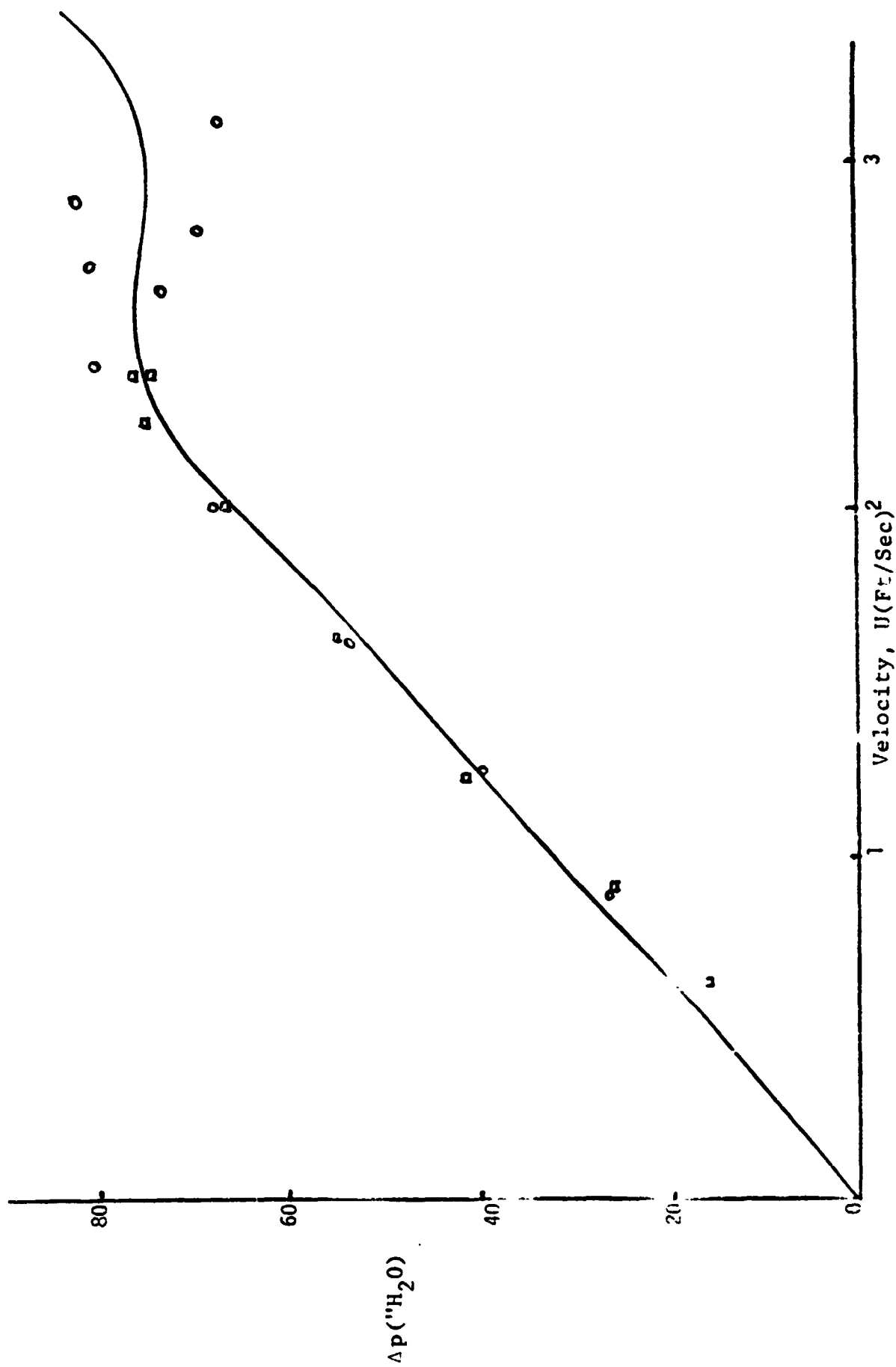


Figure 4.1
 PRESSURE DROP vs. FLOWRATE for -35/+60 MESH LEAD PARTICLES
 FLUIDIZED by HELIUM in a 2" DIAMETER COLUMN

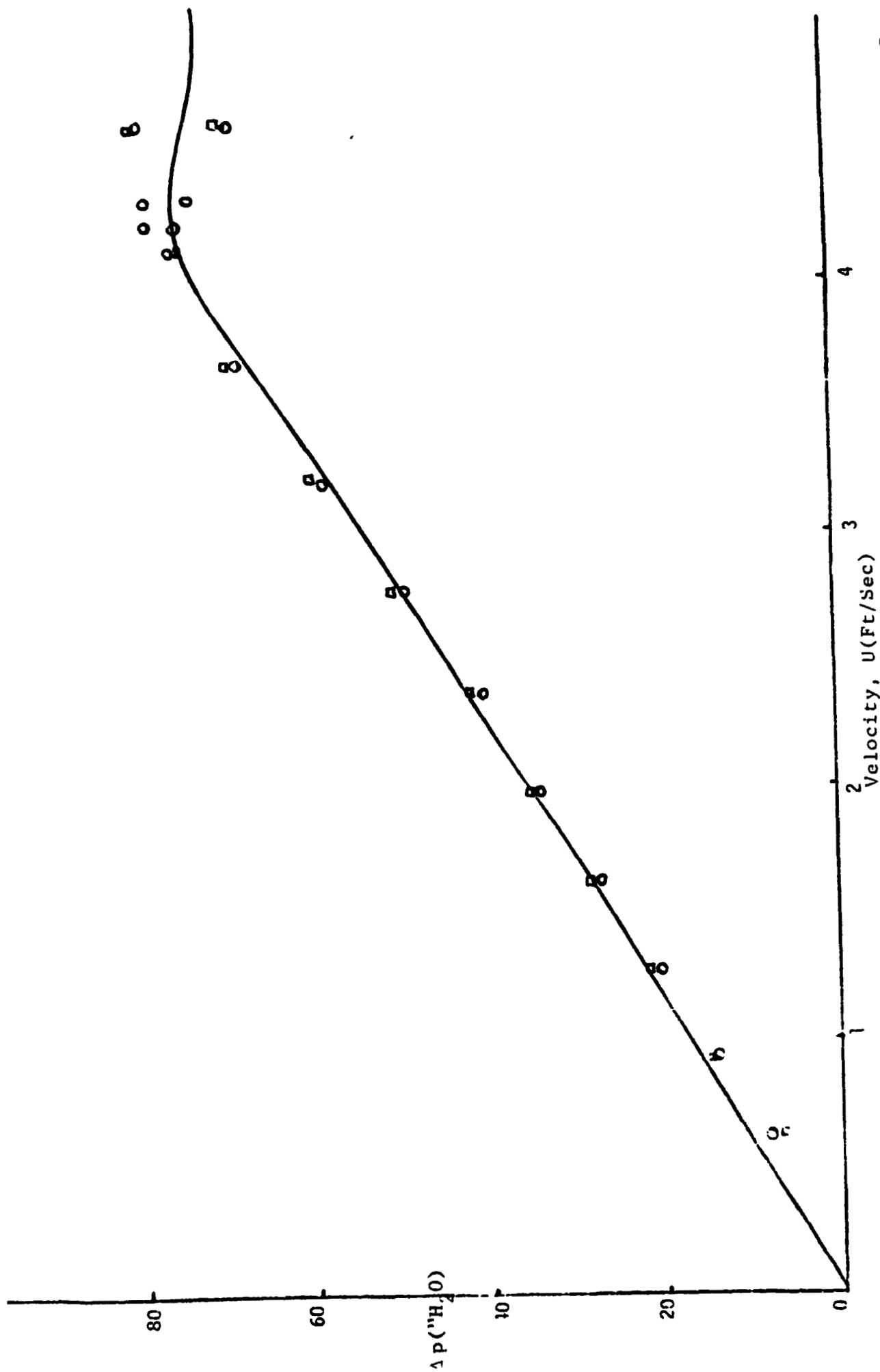


Figure 4.2
PRESSURE DROP vs. FLOWRATE for +35 MESH LEAD PARTICLES
FLUIDIZED by HELIUM in a 2" DIAMETER COLUMN

6-inch column of 2 and 1mm, respectively. The test results show a very rapid onset of slugging. With the larger particles, slugging effectively begins at the onset of fluidization.

Cold model tests in a 6-inch diameter cylinder with lead and silicon particles fluidized by helium are also in progress. The pressure drop vs flow rate measurements were made to determine the incipency of fluidization and slugging. The test results are shown in Figures 4.3 and 4.4. These tests, in conjunction with Dr. T. Fitzgerald's scaling law, suggest that a bed of 250 μ average diameter silicon particles could be operated in a 18-inch cylinder at U/U_{mf} of two or more with no slugging. However, when the average silicon particle diameter is 500 μ , some slugging would be present if the U/U_{mf} were greater than two.

4.2.2c Particle Attrition Test

In fluid-bed pyrolysis, excess silicon powder formation due to the bed motion must be avoided. On the other hand, fluid-bed pyrolysis requires replenishment of seed particles which may be produced by attrition of silicon particles. An apparatus made of a 1-inch diameter quartz tube was constructed in which silicon particles are fluidized by an inert gas.

We observed the following phenomena during brief shakedown runs at room temperature.

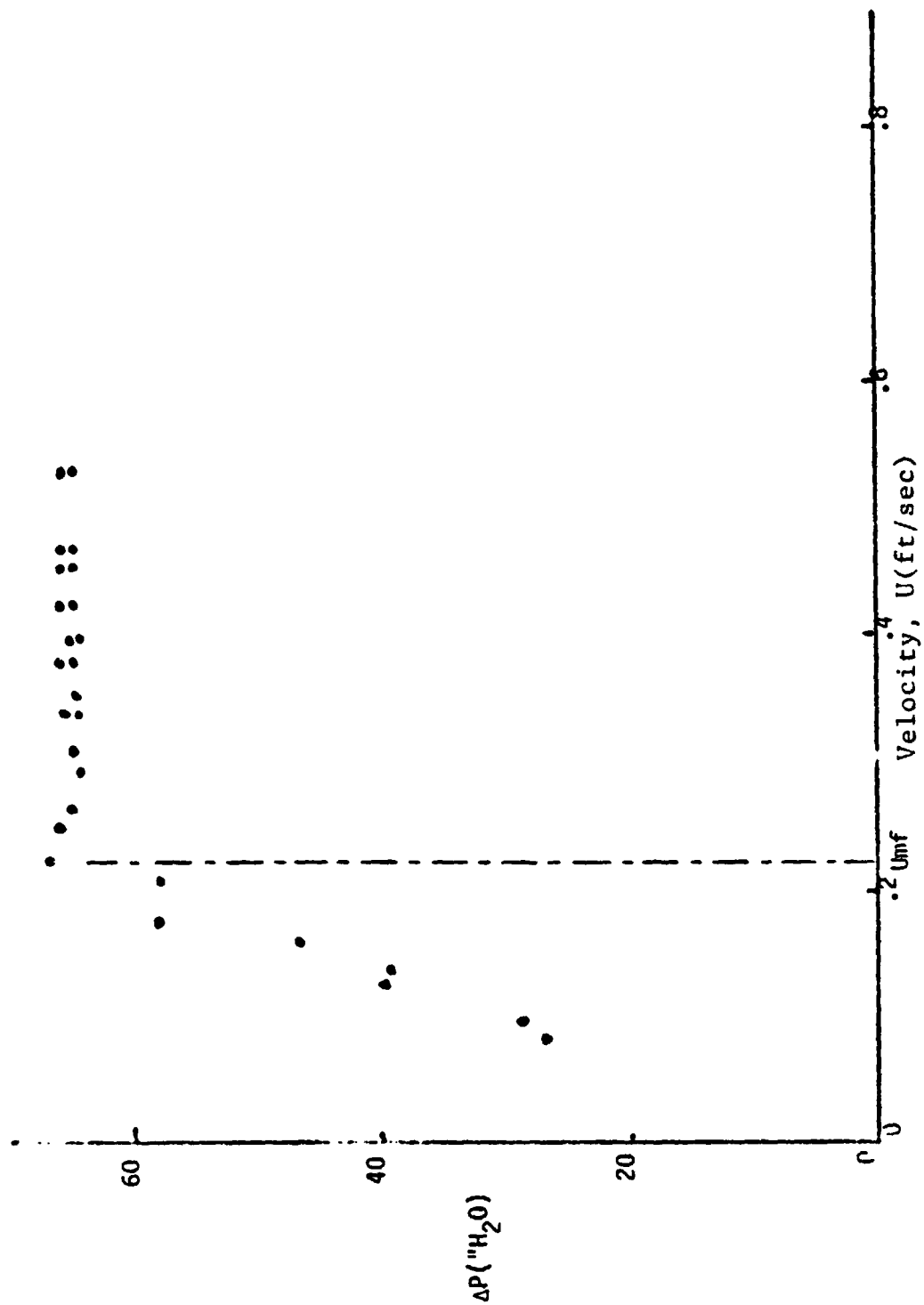


Figure 4.3

PRESSURE DROP vs. FLOWRATE for -120/+200 MESH LEAD PARTICLES
FLUIDIZED by HELIUM in a 6" DIAMETER COLUMN by 1' COLUMN

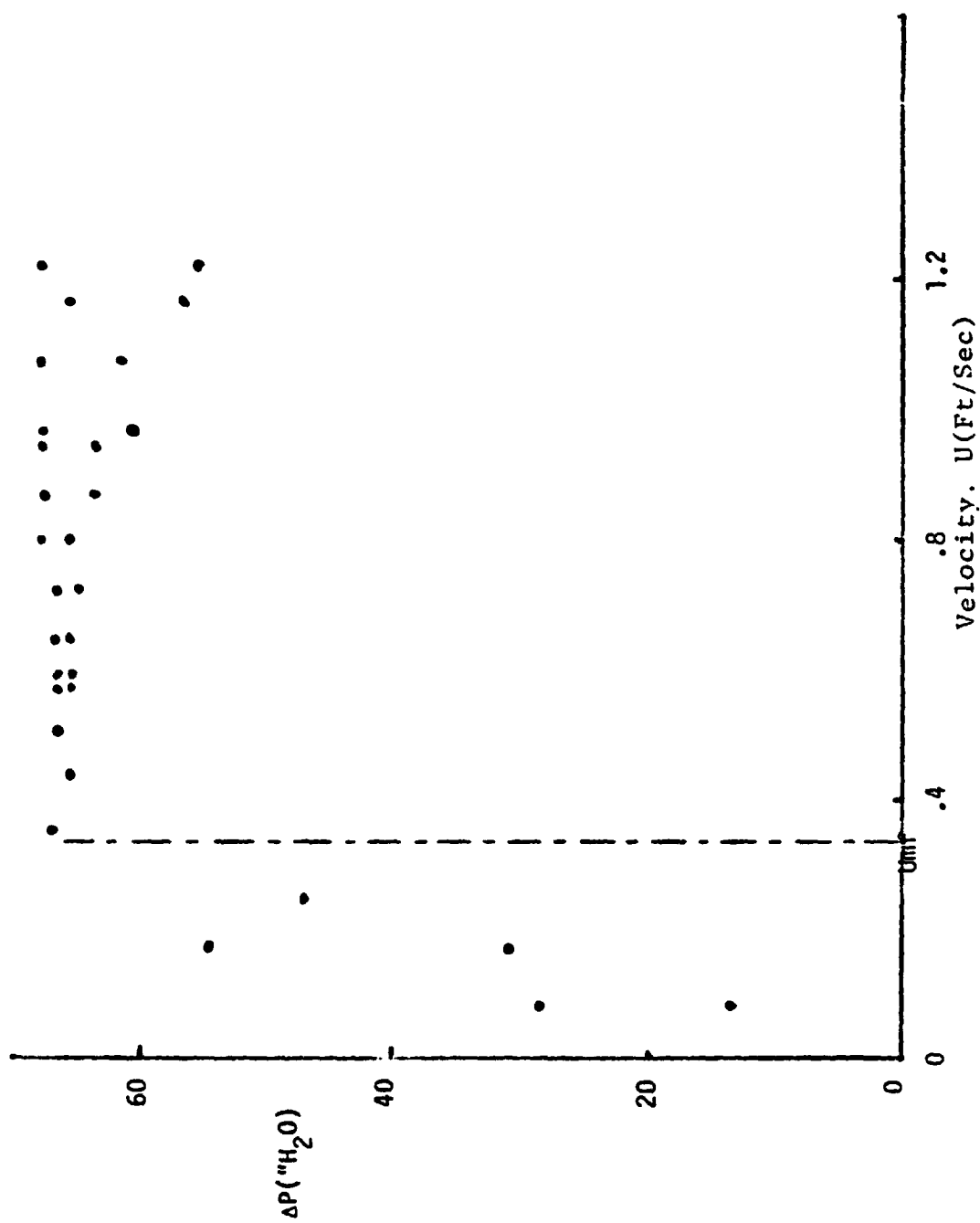


Figure 4.4

PRESSURE DROP vs. VELOCITY for $-60/+120$ MESH SILICON
FLUIDIZED by HELIUM in a 6" DIAMETER by 1' COLUMN

- . The quartz tube discolored in a characteristic manner with a brown, tightly-adhered coating occurring about one inch above the distributor. This discoloration is typical of that expected from vapor deposition or thermal effects although these causes do not exist in this case.
- . The fines generated were a very fine brown powder.

These observations suggest that it is important to distinguish between the results of mechanical abrasion and those of vapor-phase decomposition.

The rate of fines generation was measured in two beds. The first bed contained metallurgical-grade silicon particles of -35/+60 mesh at U/U_{mf} of 10. Figure 4.5 documents the rate of fines generation with time. Semiconductor-grade silicon particles were used in the second bed. These particles were found to be more prone to slugging and elutriating from the bed. The gas velocity was lowered from $10 U_{mf}$ to $5 U_{mf}$. As shown in Figure 4.6, there still was substantial fines generation. Also, rather than discoloring the walls as the metallurgical silicon did, the high-purity silicon scraped the discoloration off the walls.

4.2.3 Interim Technical Summary

The originally planned program (MOD 8) was completed on May 31, 1978, and extension work (MOD 14) was initiated in June.

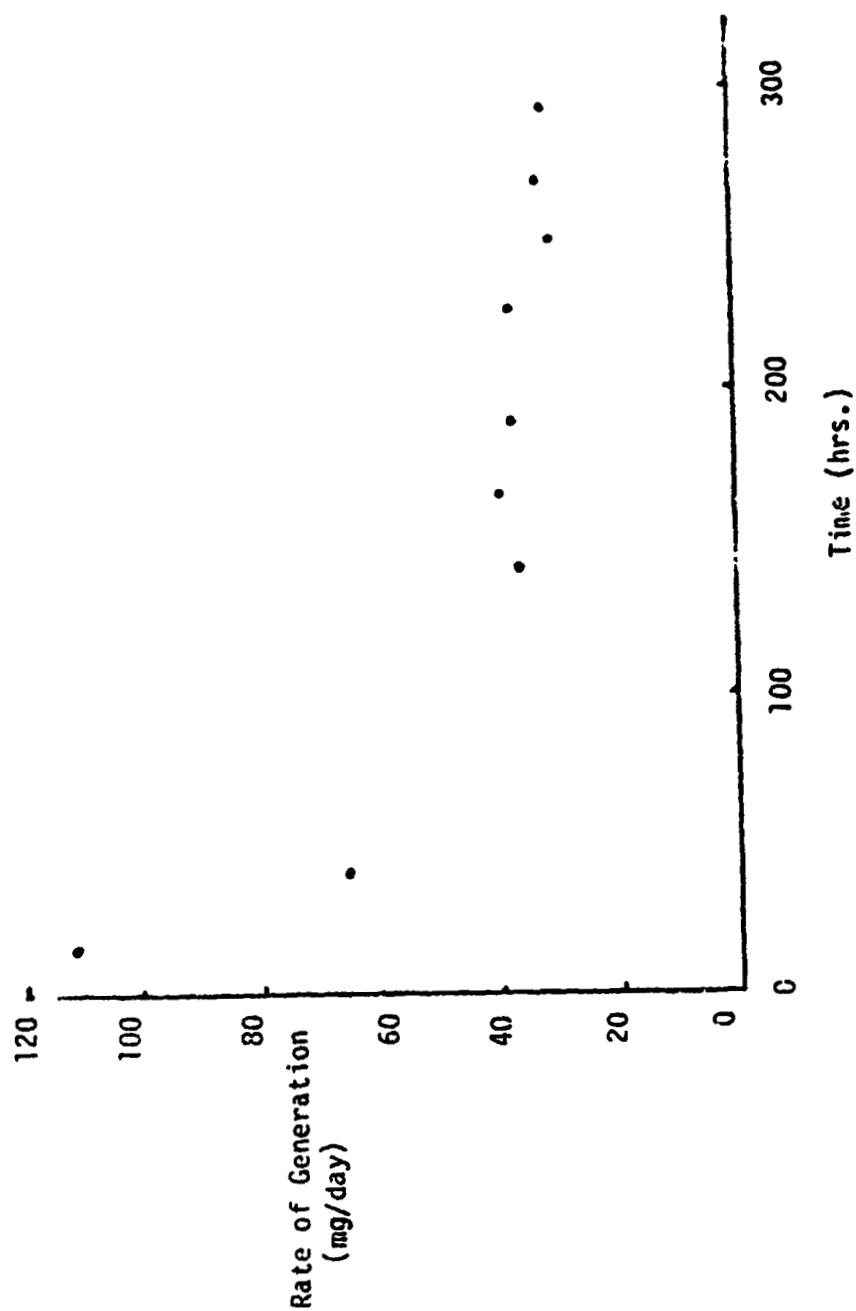


Figure 4.5
 RATE of FINES GENERATED for $-35/+60$ METALLURGICAL SILICON PARTICLES vs. TIME,
 at $U/U_{mf} = 10$, MASS of SILICON in BED = 35 GRAMS

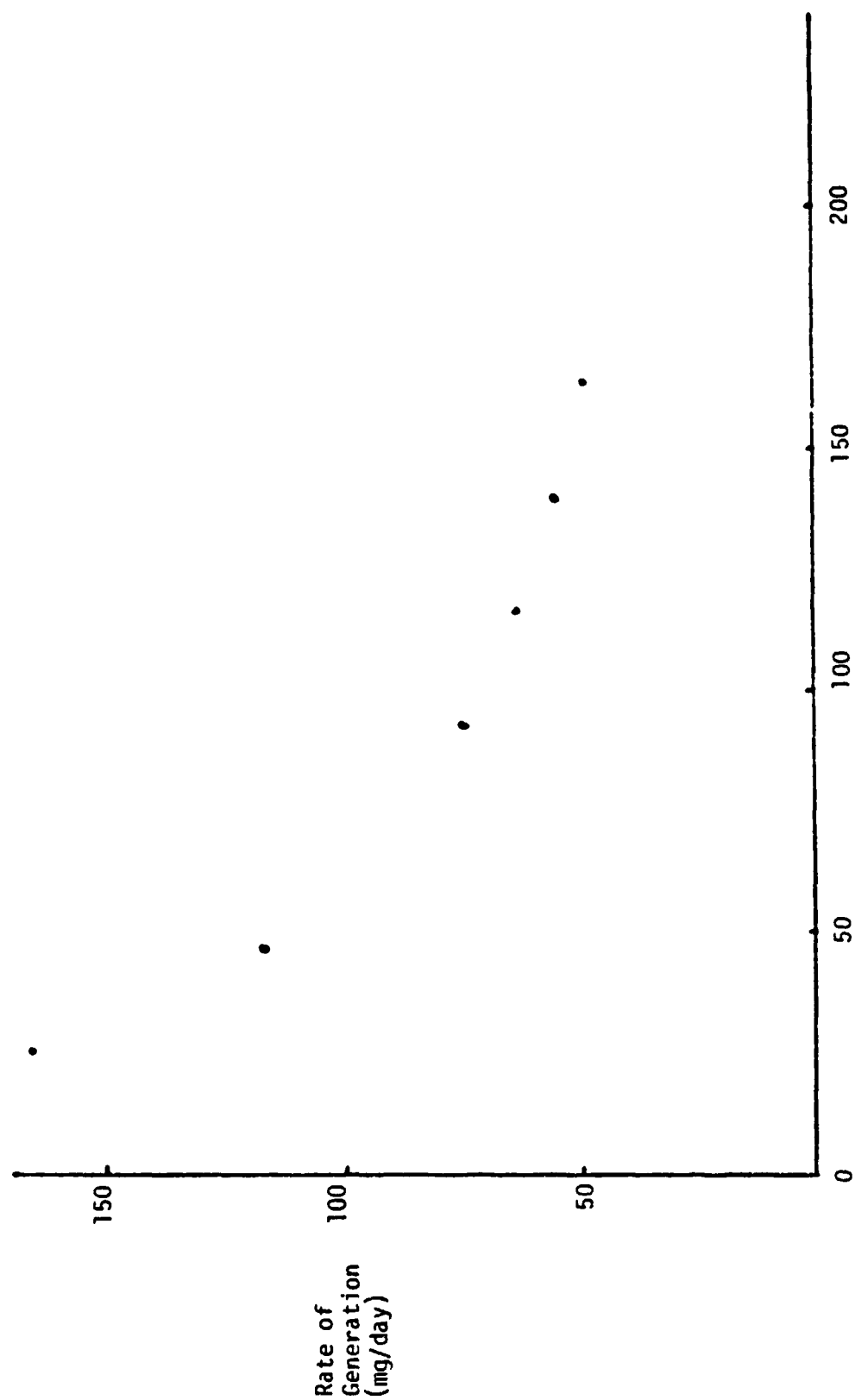


Figure 4 6
RATE of FINES GENERATION for $-35/+60$ SEMICONDUCTORS GRADE SILICON PARTICLES
at $U/U_{mf} = 5$, MASS of SILICON in BED = 35 GRAMS

An interim technical report,^(4.3) summarizing work accomplished in the first 8 months, was prepared and transmitted to JPL. The report contains the following conclusions:

- . Heating the bed particles by passing electricity through the bed is advantageous over conducting heat in through the bed walls. Conducting heat in through the walls implies that the wall and adjacent gas are hotter than the bulk of the bed, by 10-100K or more. This results in homogeneous decomposition near the wall, and encourages the coating of the wall with silicon. The wall coating will waste silicon and may shorten reactor life. It may also lead to build up of material near the wall and consequent defluidization of the bed.

The electrical bed-particle heating eliminates this unfavorable gradient and may make it possible to keep the bed walls colder than the bulk of the bed.

- . Analysis shows, on the basis of the data available, that a fluid bed can be designed that is attractive in terms of energy consumption and size if operated at low temperature (under 1000K).
- . Heating the bed by the proposed method also causes the particles to be hotter than the fluidizing gas which allows a higher inlet concentration of silane. However,

this is significant only at very high temperatures (above approximately 1150K).

- . Heat fluxes about as large as those required in a large reactor have been demonstrated experimentally at low temperature with no internal temperature gradients.
- . An unexplained transient change in the electrical characteristics of the fluid bed occurs when the voltage is first applied. This effect disappears abruptly and generally does not reappear.
- . Experiments demonstrated the principle of electrical heating with wall coating. Experiments in which gas is blown through a porous wall to prevent particle to wall contact did not work well.

4.3 Conclusions

The scaling laws advanced by Dr. Thomas Fitzgerald of Oregon State University indicate that lead particles fluidized by helium at room temperature with a 3:1 reduction in size can model 900K silicon particles fluidized by a mixture of hydrogen and silane.

Mathematical modeling of fixed-bed pyrolysis is being done. This model will be used to determine operational limits of the bed and to predict the bed performance.

A fluid-bed was successfully heated to 500°C and limited pressure drop vs flow rate measurements were made. However, a faulty transformer in the high-power equipment forced the postponement of the experiments until October.

Basic fluid-bed behavior study is conducted with 2-inch and 6-inch diameter cold beds. Test results to date suggest that a bed of 250 μ average diameter silicon particles could be operated in an 18-inch cylinder at a U/U_{mf} in excess of two with no slugging. However, when the average silicon particle diameter is 500 μ , some slugging would be present if the U/U_{mf} were greater than two.

Particle attrition tests show that high-purity silicon particles produce more fines than metallurgical-grade silicon.

4.4 Projected Quarterly Activities

4.4.1 Theoretical Investigations

4.4.1a Fluid-Bed Pyrolysis Model Update

The current fluid-bed model will be updated on the basis of the current fluidization experiments. Some backmixing effects will be included in the existing model.

4.4.1b Fixed-Bed Pyrolysis Modeling

Further calculations of fixed bed performance will be made. The current computer model works, but the computational procedure is not efficient. An improvement in the algorithm will be sought.

4.4.2 Experimental Work

4.4.2a High-Temperature Fluid-Bed

The high frequency heating experiments will continue. Heating up to 900°C will be demonstrated, and temperature differences between the bed wall and bed particles will be measured. Experiments with high purity silicon and metallurgical silicon will be made.

4.4.2b Cold Modeling Experiments

The cold, inert gas fluidization tests in the 6-inch diameter glass column will be made at reduced pressure (~2.5 to 7.5 psia). At these conditions, with helium as the fluidizing gas, the gas density and viscosity are very nearly the same as hydrogen-silane mixtures at 900K. The behavior of the cold bed should thus be very similar to that of the PDU envisioned.

4.4.2c Gas Distributor Test

Tests of the performance of a boot section as distributor will be made. The degree of segregation by particle size and the quality of gas distribution will be measured.

4.4.2d Particle Attrition Test

The attrition tests of silicon particles will be continued. Long-term tests of high and low purity silicon particles at elevated temperatures (to 900°C) will be made.